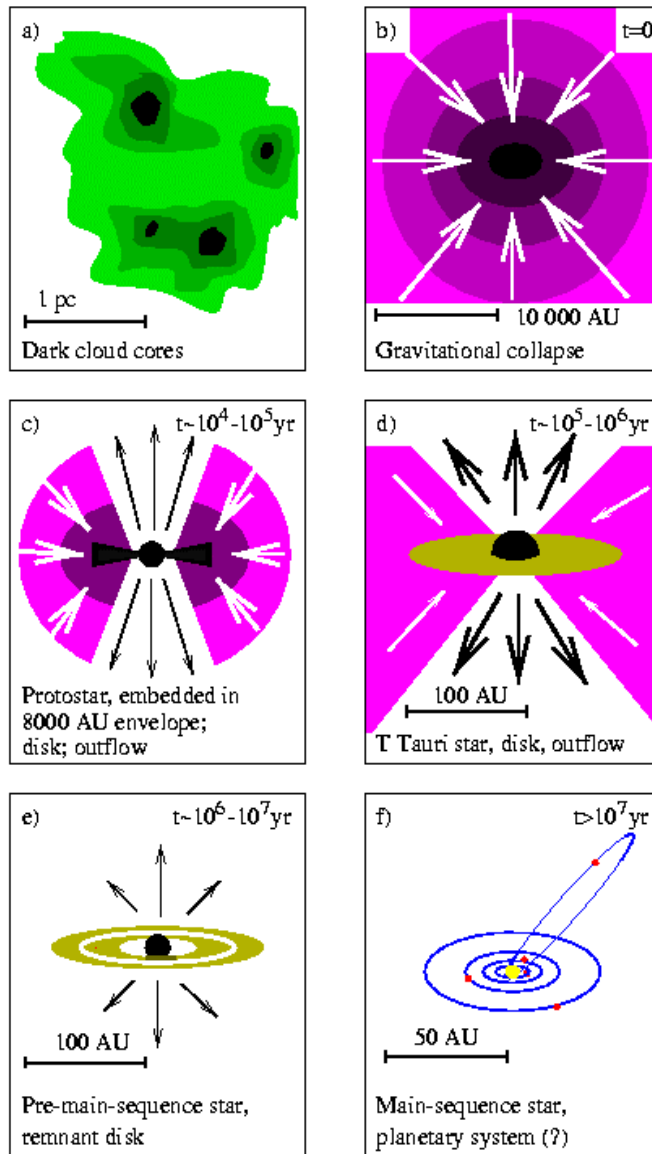


LOW MASS STAR FORMATION



Hogtheijde 1998, after Shu et al. 1987

- a) Fragmentation of cloud
- b) Gravitational contraction
- c) Accretion and ejection
- d) Formation of disk
- e) Residual disk
- f) Formation of planets

(Shu, Adams & Lizano 1987)

Formation of Massive Stars

- With great advances achieved in our understanding of low mass star formation, it is tempting to think of high mass star formation simply as an extension of low mass star formation.
- However...

Some problems with extending the picture of low-mass star formation to massive stars:

- Radiation pressure acting on dust grains can become large enough to reverse the infall of matter:

- $F_{\text{grav}} = GM_*m/r^2$

- $F_{\text{rad}} = L\sigma/4\pi r^2 c$

- *Above $10 M_{\text{sun}}$ radiation pressure could reverse infall*

So, how do stars with $M_* > 10M_\odot$ form?

- Accretion:
 - Need to reduce effective σ , e.g., by having very high M_{acc}
 - Reduce the effective luminosity by making the radiation field anisotropic
- Form massive stars through collisions of intermediate-mass stars in clusters
 - May be explained by observed cluster dynamics
 - Possible problem with cross section for coalescence
 - Observational consequences of such collisions?

Other differences between low- and high-mass star formation

- Physical properties of clouds undergoing low- and high-mass star formation are different:
 - Massive SF: clouds are warmer, larger, more massive, mainly located in spiral arms; high mass stars form in clusters and associations
 - Low-mass SF: form in a cooler population of clouds throughout the Galactic disk, as well as GMCs, not necessarily in clusters
- Massive protostars luminous but rare and remote
- Ionization phenomena associated with massive SF: UCHII regions
- Different environments observed has led to the suggestion that different mechanisms (or modes) apply to low- and high-mass SF

Still, one can think in 3 evolutionary stages:

- Massive, prestellar cold cores: Star has not formed yet, but molecular gas available (a few of these cores are known)
- Massive hot cores: Star has formed already, but accretion so strong that quenches ionization => no HII region (tens are known)
- Ultracompact HII region: Accretion has ceased and detectable HII region exists (many are known)

Ultracompact HII Regions

- Because they are the best studied (and easiest to detect), we start with the latest stage, the UCHIIs, and go backward in time.
- Small (diameter $< 10^{17}$ cm), dense ($n_e > 10^4$ cm $^{-3}$), and bright (EM $> 10^7$ pc cm $^{-6}$) HII regions, ionized by OB stars and deeply embedded in molecular clouds

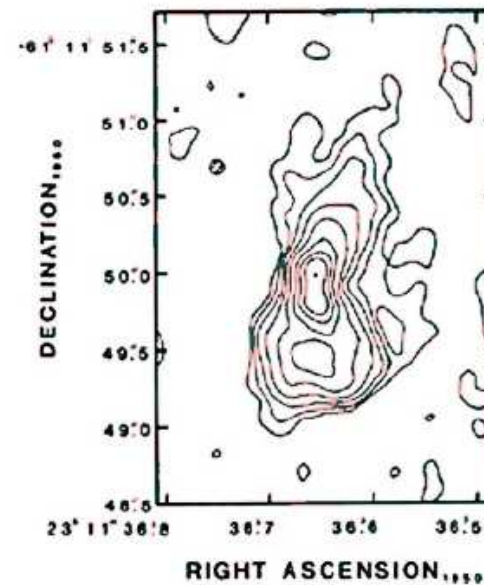
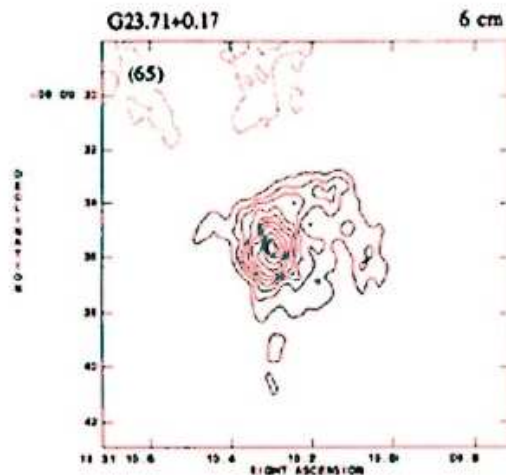
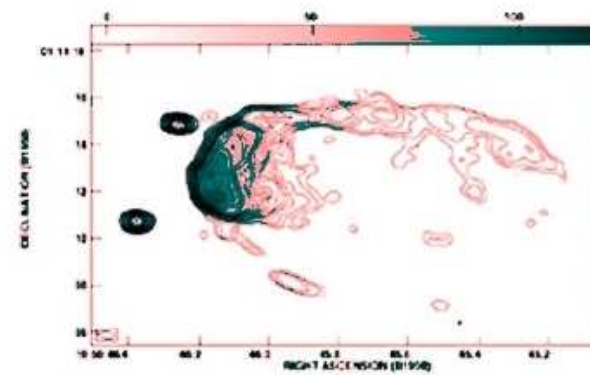
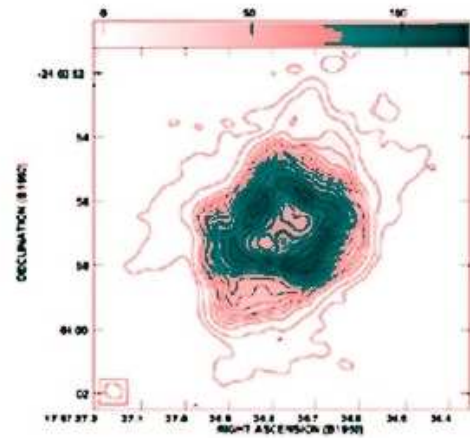


Figure 8 Examples of UC HII morphological types. Top left: G5.89 – 0.39, a shell-like structure. Top right: G34.26 + 0.15, a cometary nebula. Lower left: G23.71 + 0.17 from Wood & Churchwell (1989a), a core/halo morphology. Lower right: NGC7538 IRS1 from Campbell (1984), a bipolar nebula.

Morphologies are a reflection of the conditions of the dense gas from which they formed.

The lifetime problem

- Early studies by Wood & Churchwell (1989) suggested a large number of UCHII in the galaxy. Combining VLA and IRAS observations, estimated some 1,000 UCHII in the galaxy ionized by an O star.
- However, lifetime of HII region as UC should be of order 10^4 years and assuming 1 O star forms every 100 year, you would expect only about 100 UCHII in the galaxy.
- Factor of 10 discrepancy.

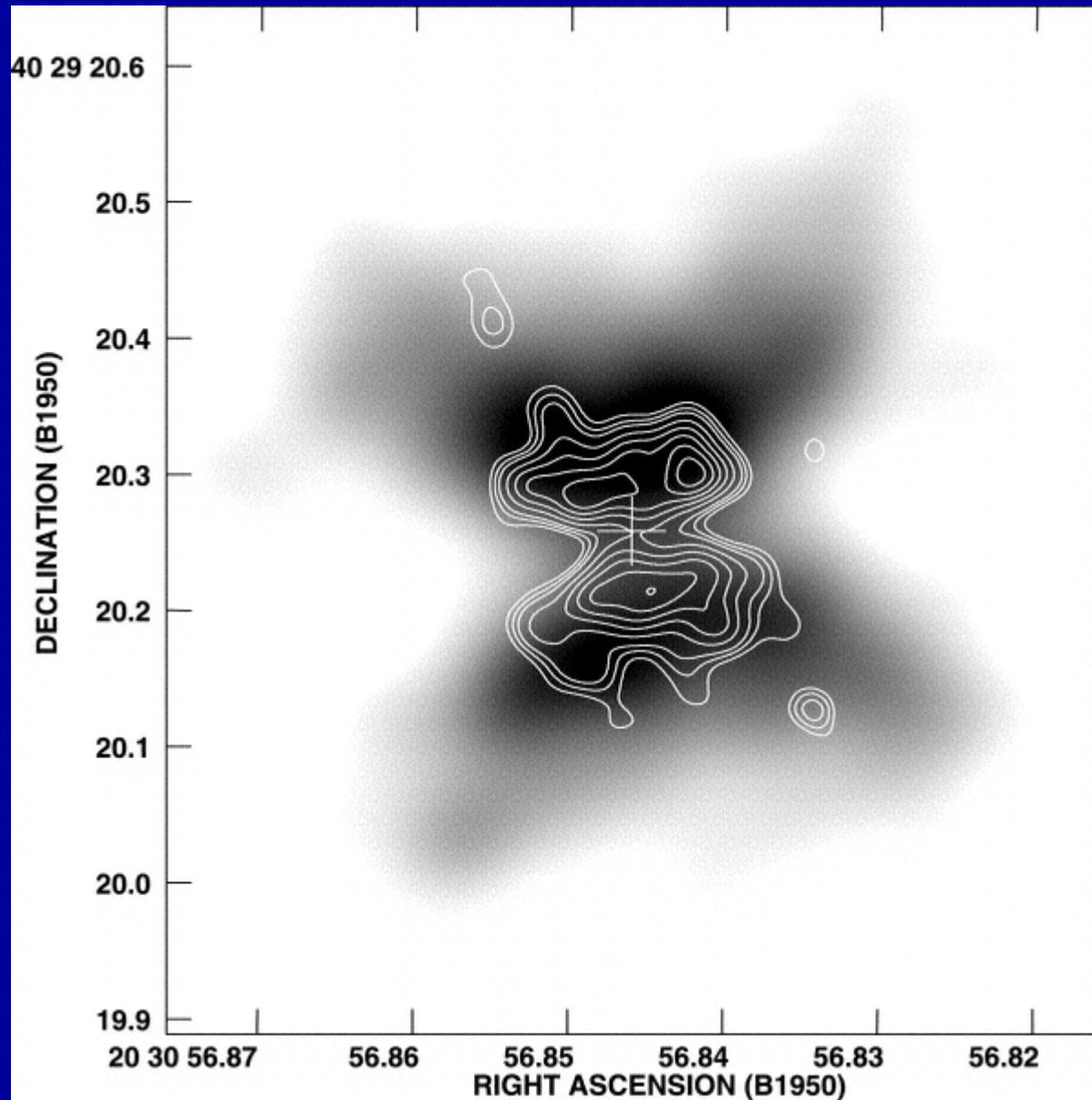
* The numbers I use are only approximated

Solutions fall into two categories:

1. Mechanisms to extend the lifetime

- Infalling matter (unstable)
- Bowshocks (too fast stellar motions)
- Mass loaded flows (very inhomogeneous gas)
- Photoevaporating disks (few sources similar to MWC 349)

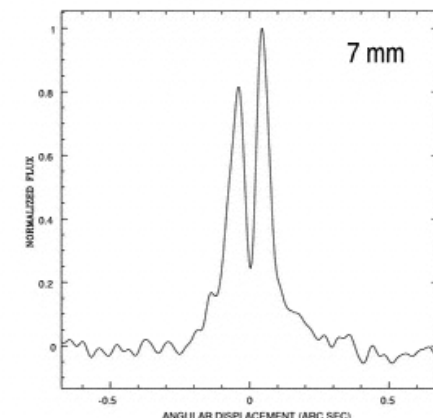
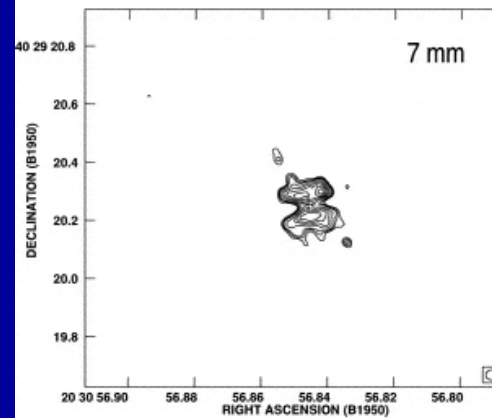
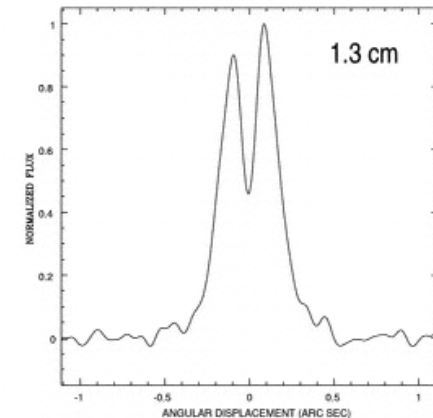
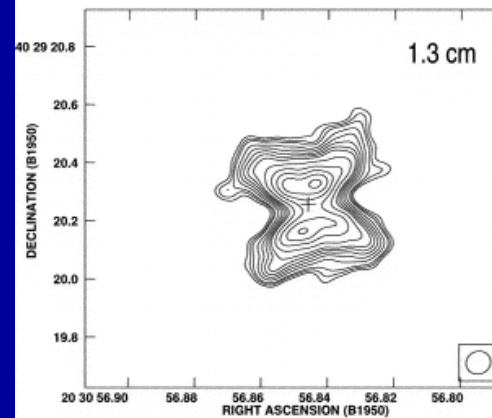
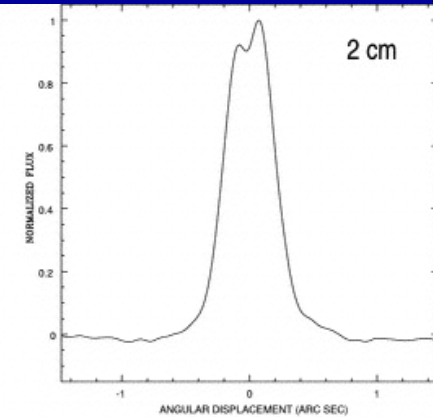
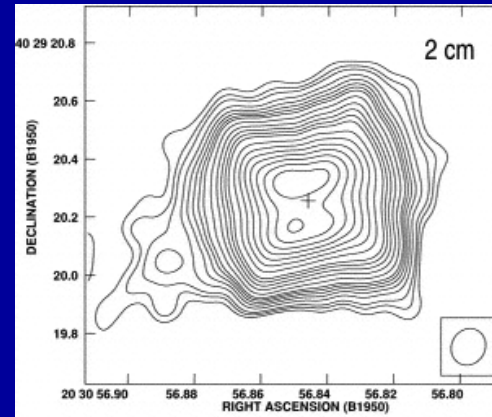
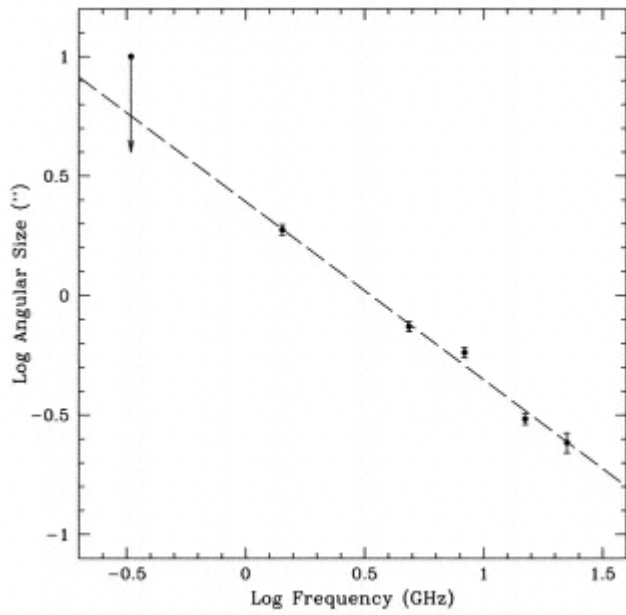
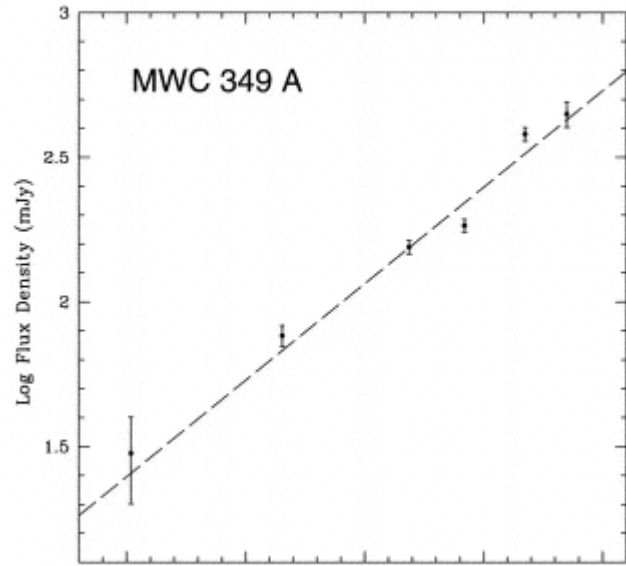
MWC 349: A photoevaporating disk (Tafoya et al. 2004)



VLA observations

Greyscale: 2 cm

Contours: 7 mm



Tafoya et al. (2004)

Solutions fall into two categories:

2. Something wrong with assumptions

- External molecular gas much denser (10^7 cm^{-3}) than used by WC89
- Turbulence in molecular gas will help confinement
- At present there is still no consensus on the explanation

Time Variation in UCHIIs

- Hydrogen recombination time is of order $1/(n_e \alpha_B)$, where α_B is recombination rate to levels $n \geq 2$. $\alpha_B = 2.6 \times 10^{-13}$ for $T_e = 10^4$ K. For n_e of order 10^5 and larger, recombination times a year or less.
- Can we see variation in UCHIIs?

Recombination Time

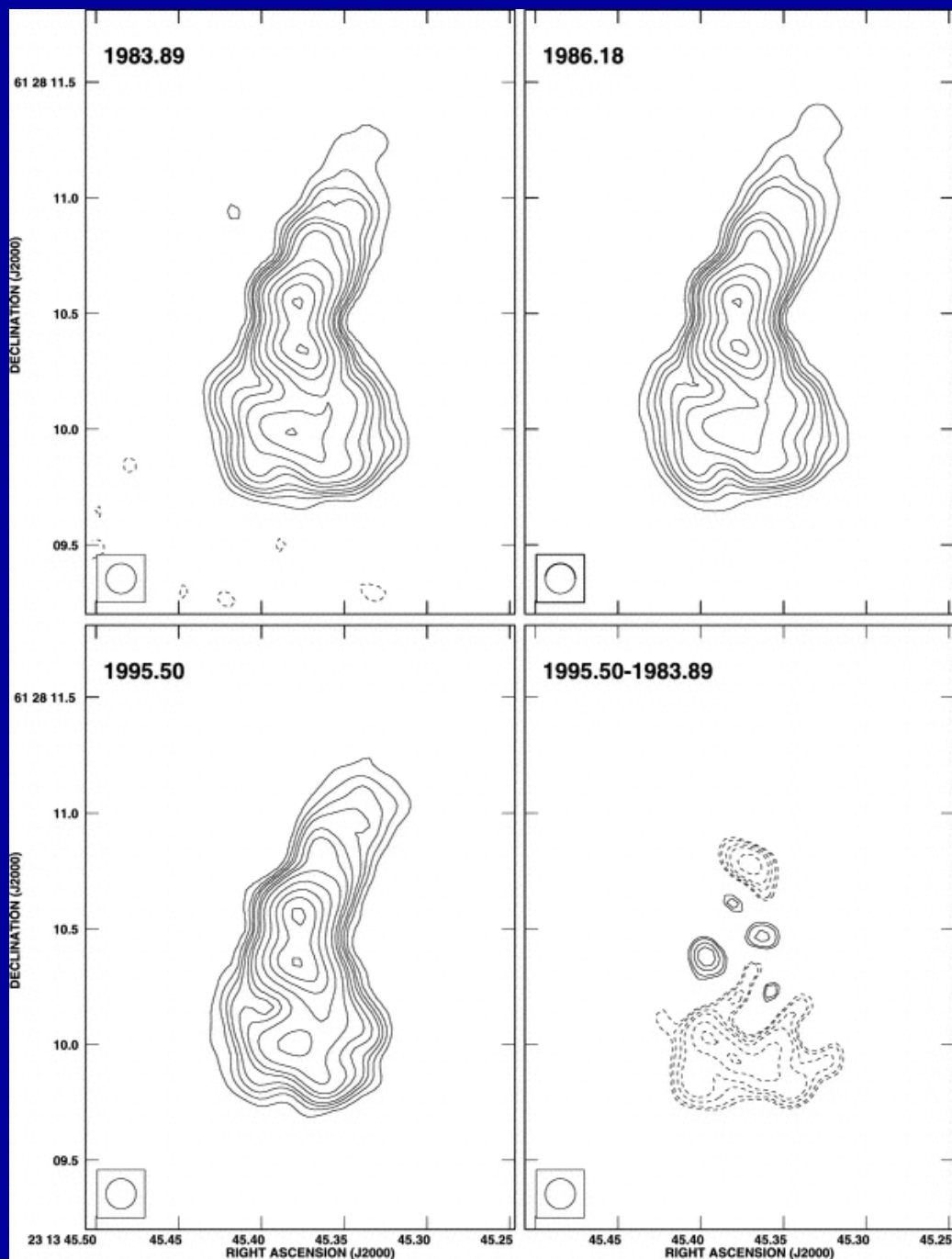
- Ionized region with initial electron density given by $n_e(0)$ at $t=0$. Turn off source of ionization.

$$\frac{dn_e}{dt} = -\alpha_B n_e^2 \quad \text{solves to}$$

$$n_e(t) = n_e(0) \frac{1}{1 + \alpha_B n_e(0)t}$$

Original ionization drops to $1/2$ after

$$t_{rec} = \frac{1}{\alpha_B n_e}$$



NGC 7538 IRS1

Bipolar UCHII

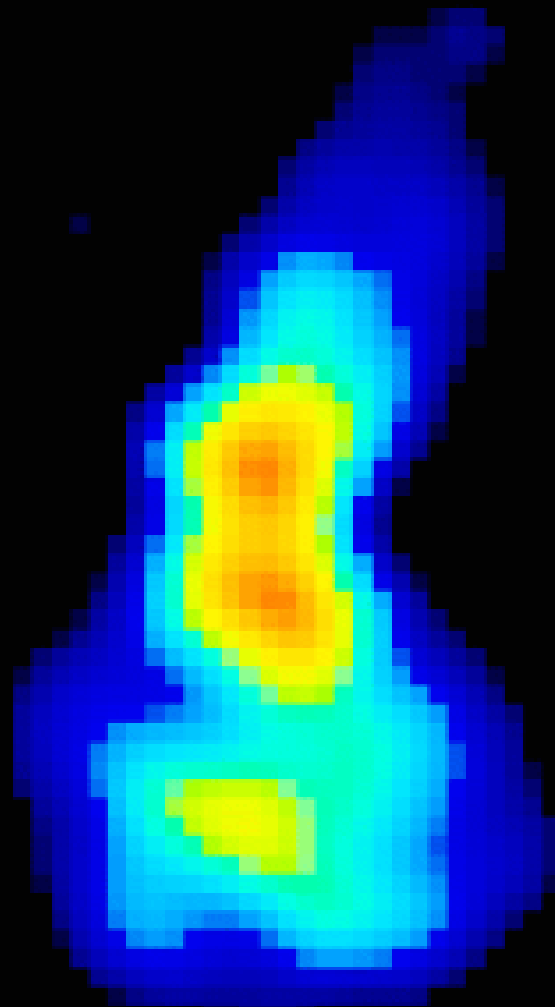
Methanol disk of
Pestalozzi et al. (2004)

Archival VLA
observations at 2 cm made
over decades

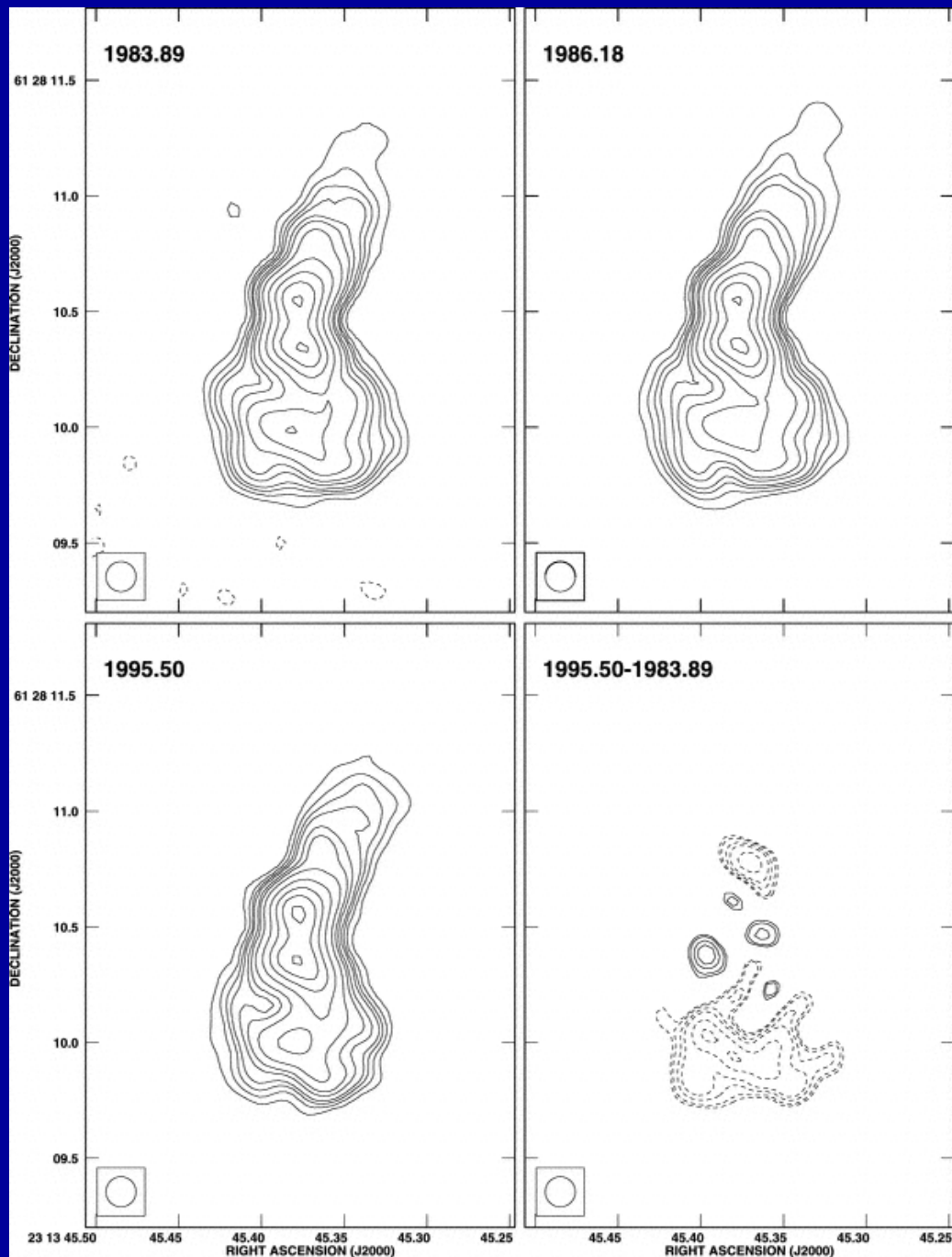
Franco & Rodriguez
(2004) find variations in
lobes (secular decrease)

Core is optically thick and
does not seem to be
varying much (it could be
varying, but since optically
thick, we cannot say

NGC 7538 IRS1



1983.9



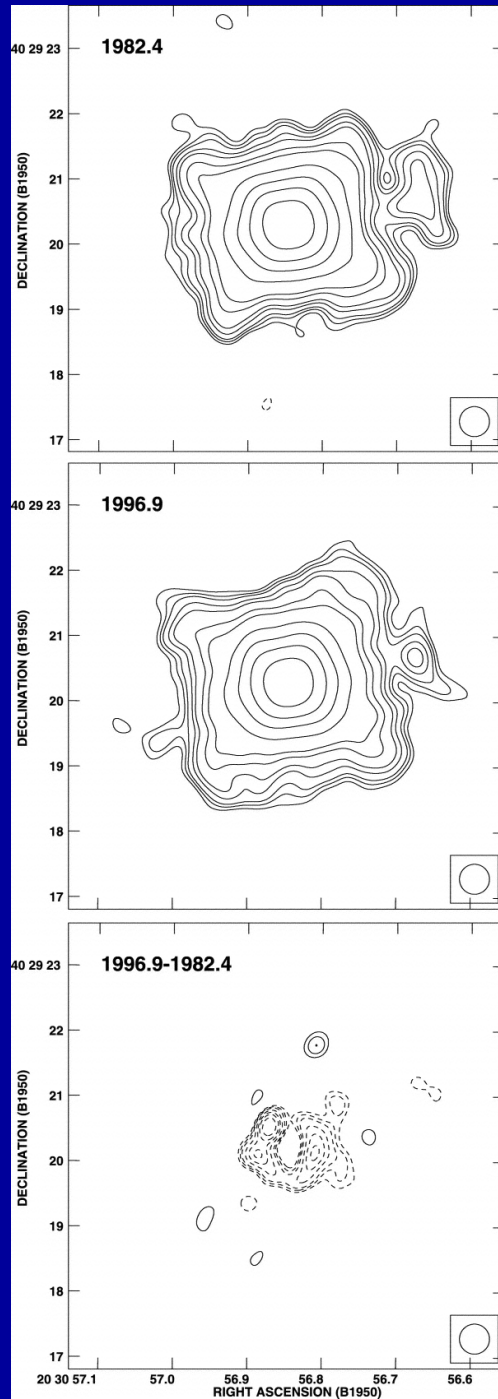
NGC 7538 IRS1

Possible explanations for variability:

Ionizing flux from star is decreasing (unlikely)

Injection of fresh gas in core “steals” ionizing photons for the lobes

Millimeter observations (where all nebula is optically thin) will help clarify situation.



MWC 349 (the photoevaporating disk)
also seems to be varying with time

Tafoya et al. (2004)

Let's go back in time to the Hot
Molecular Core (HMC) stage

PHYSICAL PARAMETERS OF HOT MOLECULAR CORES

| | |
|-------------|---------------------------|
| Diameter | $\lesssim 0.1 \text{ pc}$ |
| Mass | $10 - 10^4 M_{\odot}$ |
| Temperature | $> 100 \text{ K}$ |
| Density | $> 10^7 \text{ cm}^{-3}$ |

Also quite luminous, $L \geq 10^4 L_{\text{sun}}$, since star
already formed

Table 1: Known hot cores and their physical parameters. Mass and luminosity estimates are derived respectively from (sub)millimeter continuum emission and from infrared flux densities.

Table 1

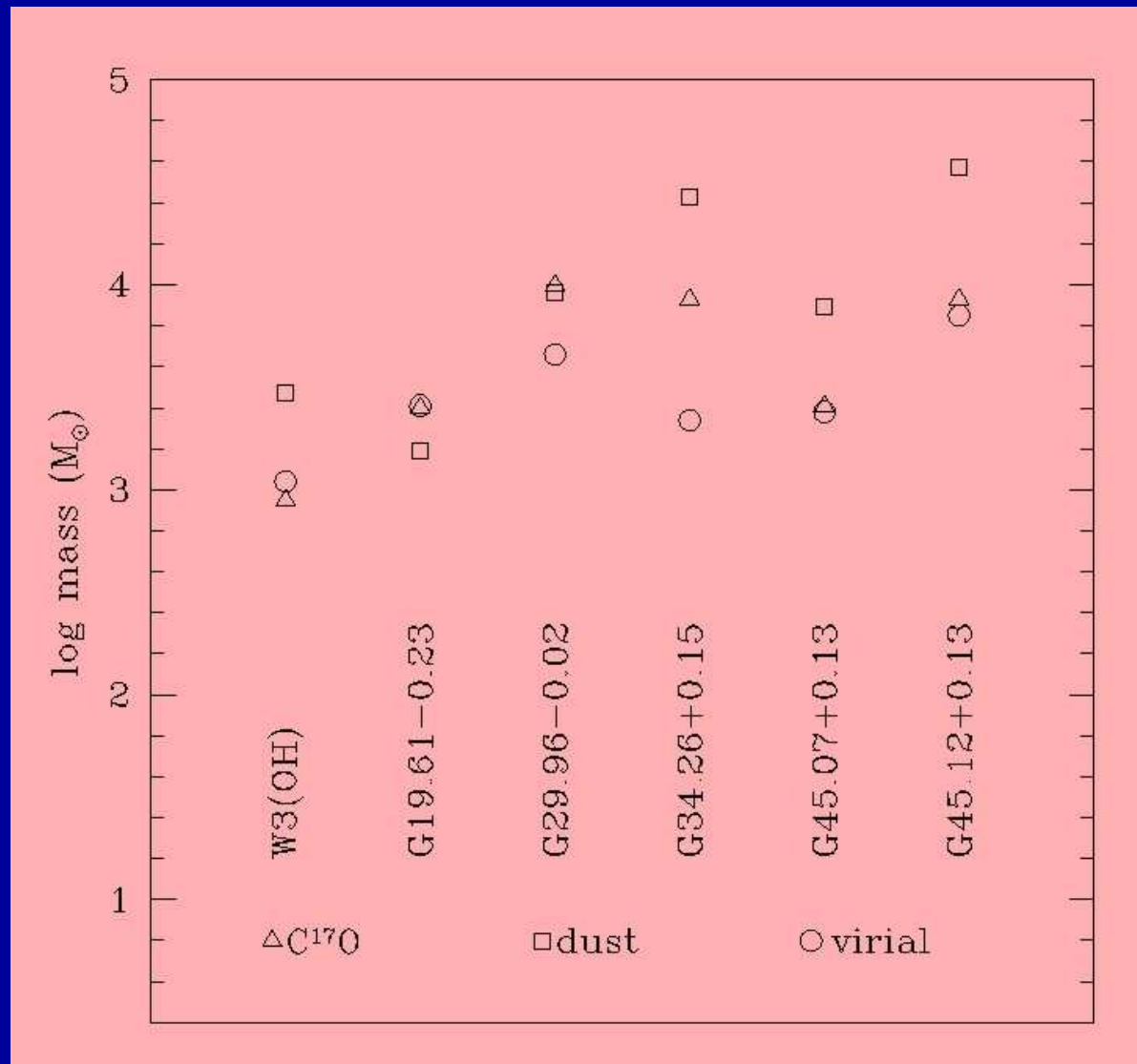
| Source Name | Dist. (kpc) | T_{kin} (K) | Diarn. (pc) | Mass (M_{\odot}) | L_{IR} (L_{\odot}) | Ref. code |
|--------------------------|-------------|---------------|-------------|----------------------|--------------------------|-----------|
| Orion-KL | 0.5 | 300 | 0.05 | 10 | $1.0 \cdot 10^5$ | 1 |
| SgB2N ^a | 8.5 | 200 | 0.1 | 2000 | $6.5 \cdot 10^6$ | 2 3 |
| SgB2M ^a | 8.5 | 200 | 0.1 | 2000 | " | 2 |
| G5.89-0.39 ^a | 4.0 | 90 | 0.18 | 2800 | $7.1 \cdot 10^5$ | 4 5 |
| G9.62+0.19 | 5.7 | >100 | 0.059 | 55-160 | $4.4 \cdot 10^5$ | 6 7 |
| G10.47+0.03 ^a | 5.8 | 150 | 0.078 | 2200 | $5.0 \cdot 10^5$ | 6 8 9 10 |
| G10.62-0.38 ^a | 6.0 | 144 | 0.05 | 1100 ^b | $1.1 \cdot 10^6$ | 11 12 |
| G19.62-0.23 | 3.5 | 230 | 0.032 | 450 | $1.6 \cdot 10^5$ | 13 |
| G29.96-0.02 | 7.4 | 100 | 0.052 | 460 | $1.4 \cdot 10^6$ | 6 8 14 |
| G31.41+0.31 | 7.9 | 110 | 0.080 | 2500 | $2.6 \cdot 10^5$ | 6 8 9 |
| G34.26+0.15 | 3.8 | 250 | 0.066 | 1400 | $6.3 \cdot 10^5$ | 4 15 16 |
| | | | | | | 17 18 |
| G45.07+0.13 ^a | 8.3 | 140 | 0.027 | <7800 | $1.1 \cdot 10^6$ | 19 |
| G45.12+0.13 ^a | 8.3 | 120 | 0.056 | <37000 | $1.3 \cdot 10^6$ | 19 20 |
| G45.47+0.05 ^a | 8.3 | 90 | 0.056-0.3 | 250 | $1.1 \cdot 10^6$ | 20 |
| IRAS 20126+4104 | 1.7 | 200 | 0.012 | 10 | $1.3 \cdot 10^4$ | 21 |
| DR21(OH) MM1 | 3.0 | >80 | 0.05 | 350 | $5.0 \cdot 10^4$ | 22 23 |
| W3(H ₂ O) | 2.2 | 220 | 0.014 | 10 | $1.0 \cdot 10^5$ | 24 |
| W51 e2 ^a | 8.0 | 140 | 0.093 | 200-400 | $1.5 \cdot 10^6$ | 25 26 |
| W51 e8 ^a | 8.0 | 130 | 0.096 | <200 | " | 25 26 |
| W51 N-Dust | 8.0 | 200 | 0.1 | 400 | " | 25 26 |

^a with embedded UC HII region

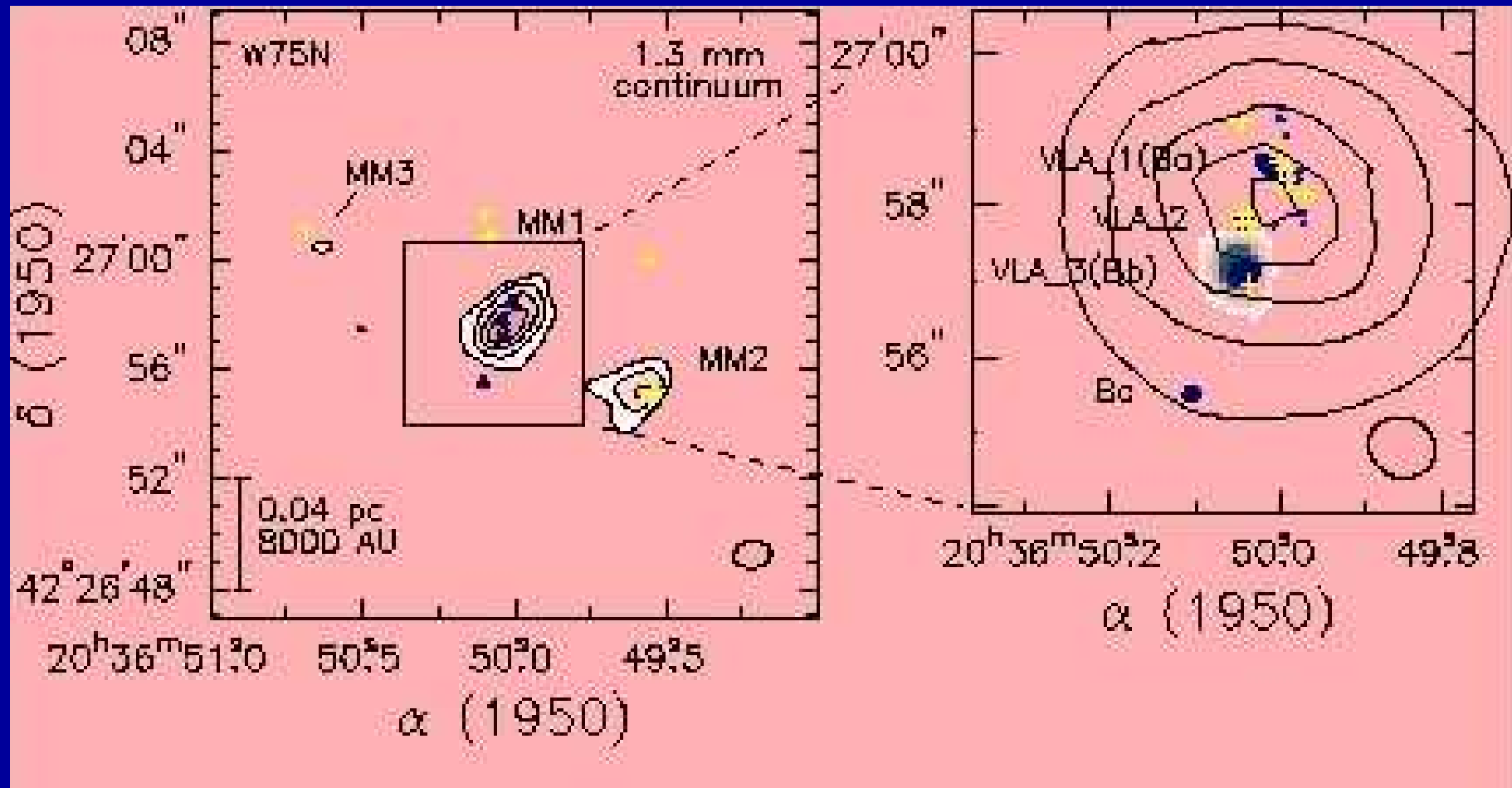
^b derived from C¹⁸O

References: (1) Wright et al. 1996. (2) Wilson et al. 1996. (3) Peng et al. 1993. (4) Akeson and Carlstrom 1996. (5) Gómez et al. 1991. (6) Cesaroni et al. 1994a. (7) Hofner et al. 1996. (8) Cesaroni et al. 1998. (9) Olmi et al. 1996b. (10) Garay et al. 1993 (11) Ho et al. 1994. (12) Keto et al. 1988. (13) Cesaroni pers. comm. (14) Hofner et al. in prep. (15) Millar, Macdonald and Gibb 1997 (16) Hunter et al. 1998 (17) Garay et al. 1990 (18) Heaton et al. 1989 (19) Hunter et al. 1997. (20) Hofner et al. 1998. (21) Cesaroni et al. 1997. (22) Mangum et al. 1991. (23) Mangum et al. 1992. (24) Wyrowski et al. 1997. (25) Zhang and Ho 1997. (26) Zhang et al. 1998.

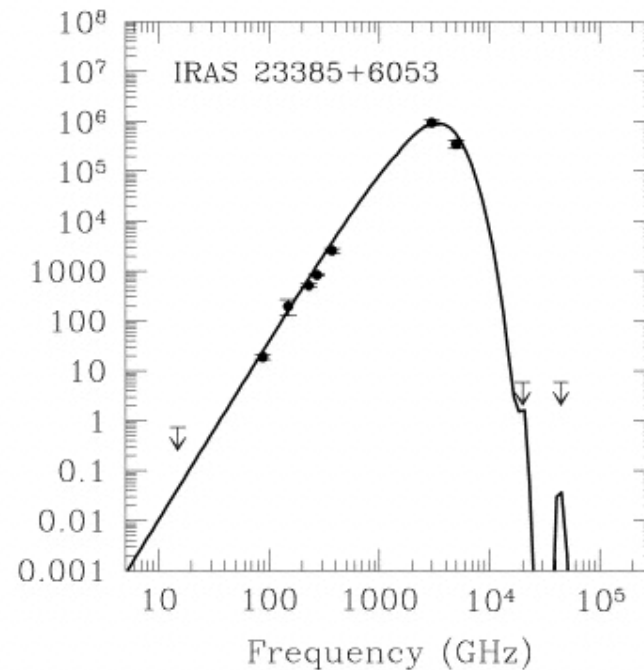
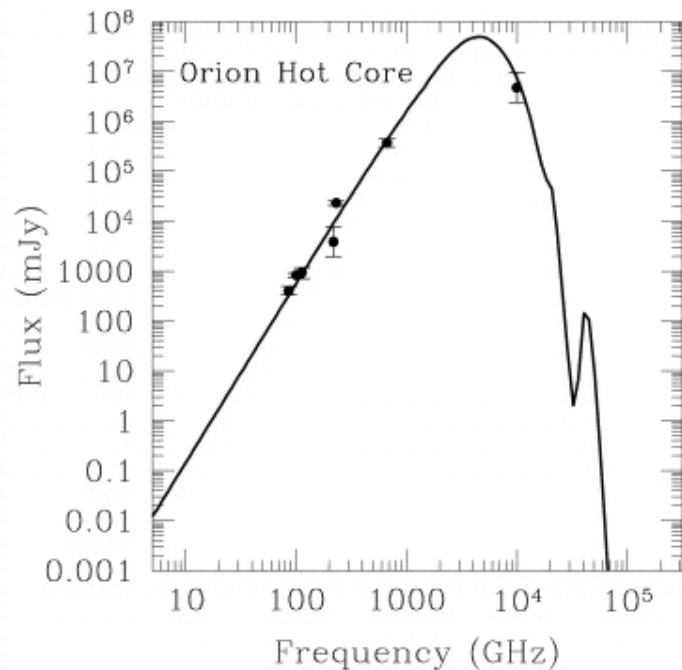
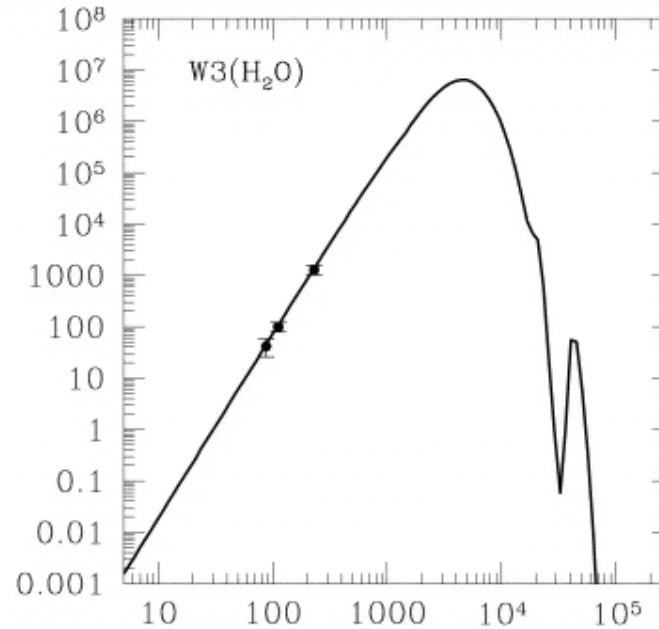
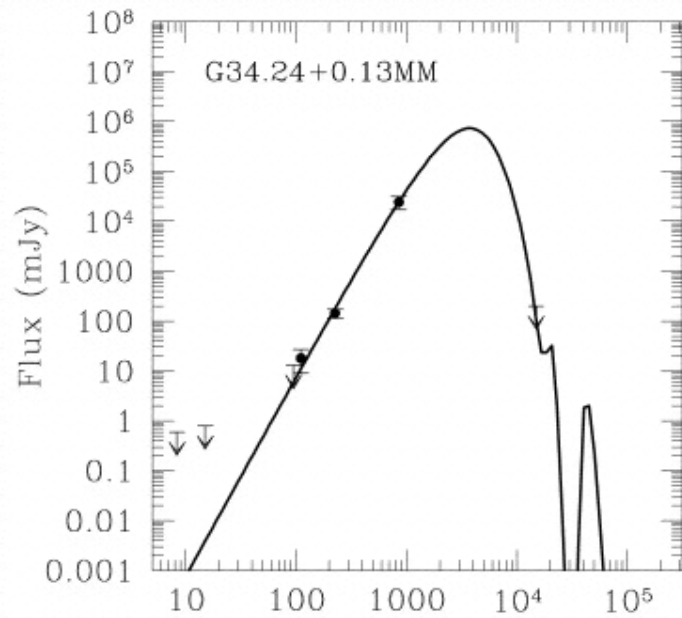
Kurtz et al. (2000)



Mass determinations from molecules, dust and virial theorem agree within an order of magnitude



W75N HMC, contours = NH₃, greyscale = continuum,
 + = H₂O masers. Three star formation sites embedded in one HMC



Osorio et al.
(1999)

Models of
continuum
emission from
HMCs

Chemistry
discussed by
Charnley

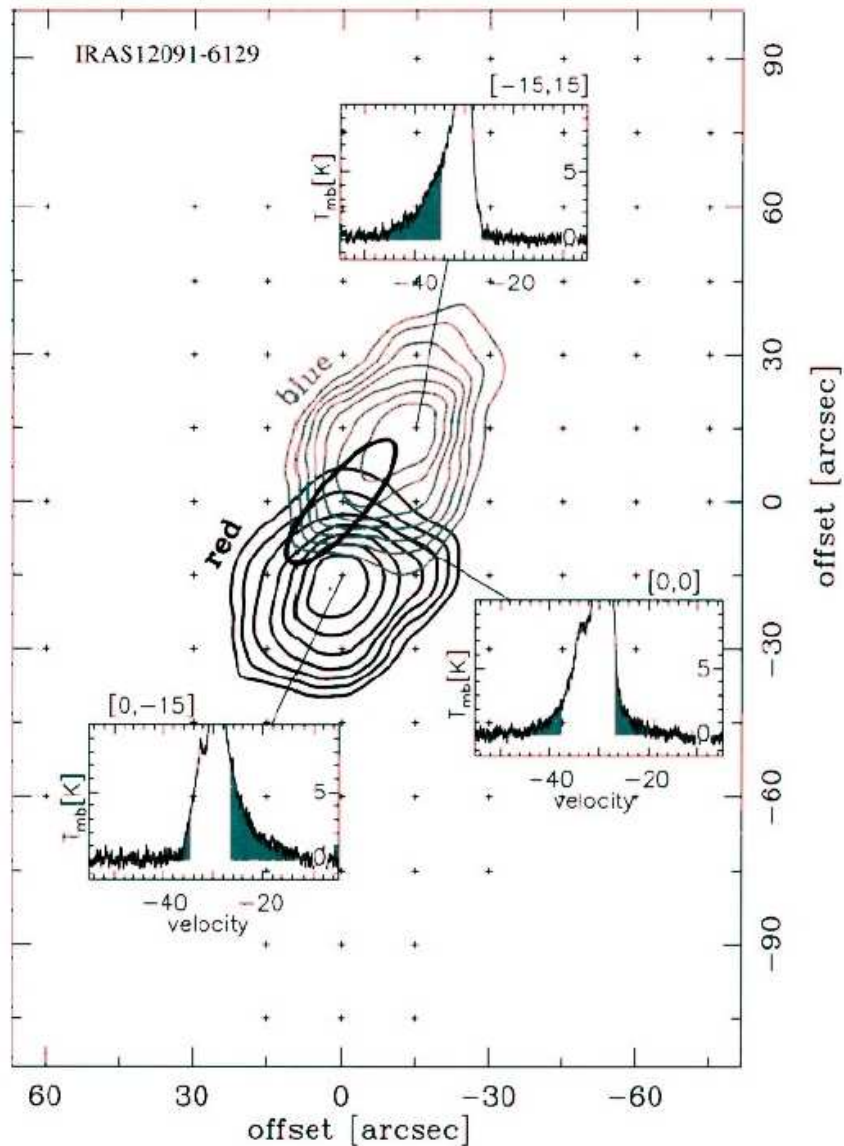


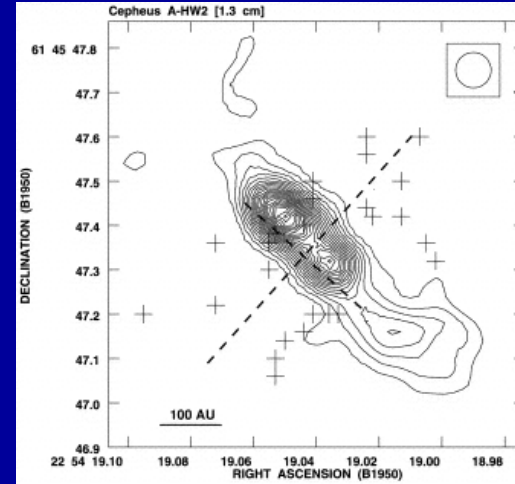
Figure 6 The CO outflow presumably driven by the FIR source IRAS12091-6129 from Henning et al. (2000). This figure illustrates three general properties of outflows driven by massive protostars: low outflow speeds, poor collimation, and large masses. The arbitrary cutoff velocities (shaded regions in the spectra) for the outflow also illustrate why outflow masses are uncertain and different authors disagree on the estimated masses.

In the HMC stage, it is frequent to find molecular outflows associates with the embedded stars. These outflows disappear by the UCHII stage.

Molecular outflows from massive protostars are believed to be more massive, but slower and less collimated than outflows from low mass stars. However, some sources well collimated.

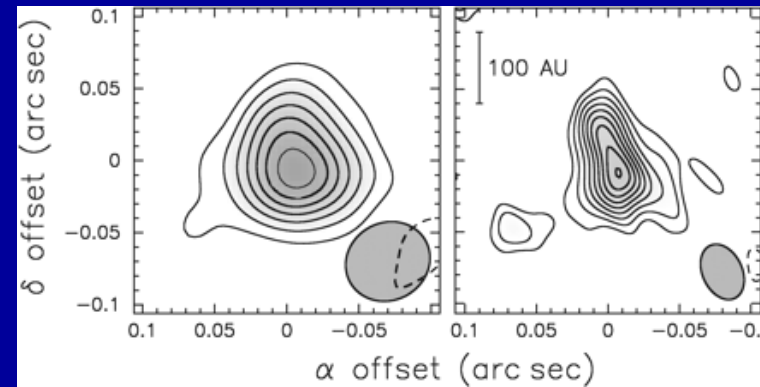
B STARS

- **Cepheus A HW2**
(Rodríguez et al. 1994)



- **IRAS 20126+4104**
(Cesaroni et al. 1997; Zhang et al. 1998)

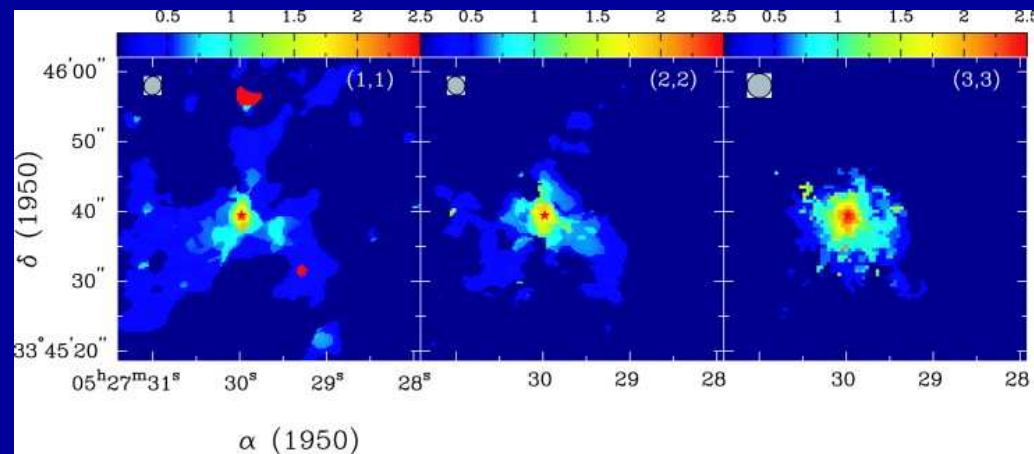
- **G129.16-3.82**
(Shepherd et al. 2001)



- **AFGL 5142**
(Zhang et al. 2002)

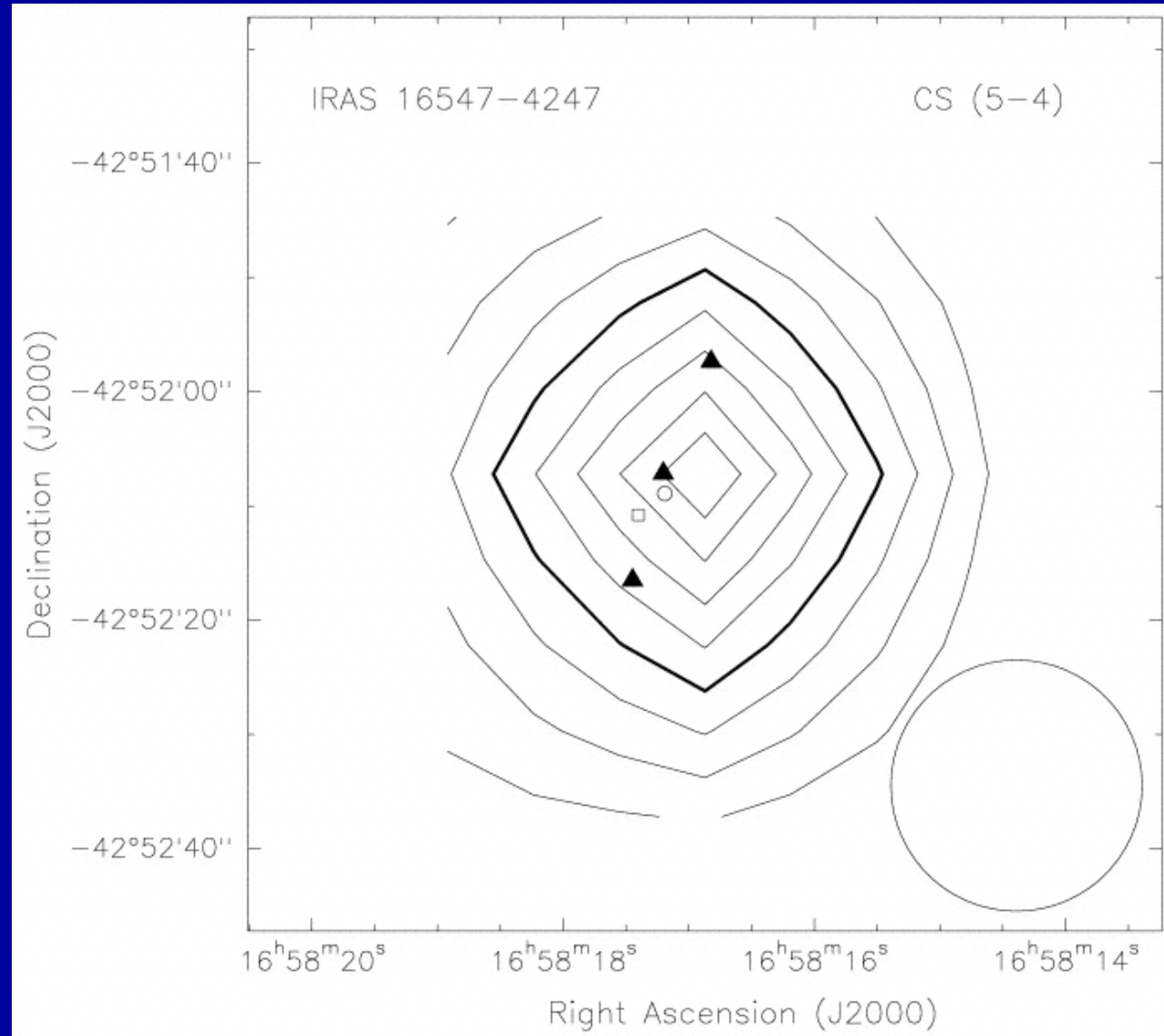


- **AFGL 2591**
(Trinidad et al. 2003)



O STARS

- IRAS 16547-4247
(Garay et al. 2003)



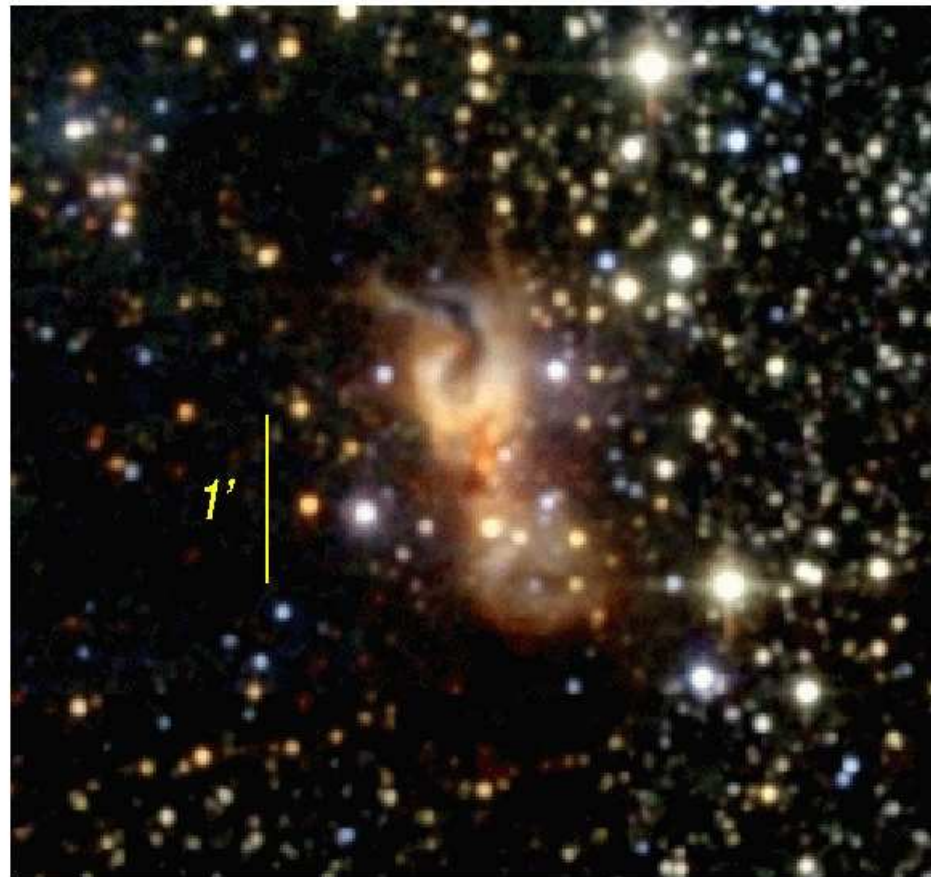
HH 80-81 (GGD27)
in L291 dark cloud

Distance 1.7 kpc
(Rodríguez et al. 1980),

Luminosity: 2×10^4
 L_{Sol}

Star: B0.5 ZAMS

Two Micron All Sky Survey



HH 80-81 also known as GGD 27 (Gyulbudaghian et al. 1978)

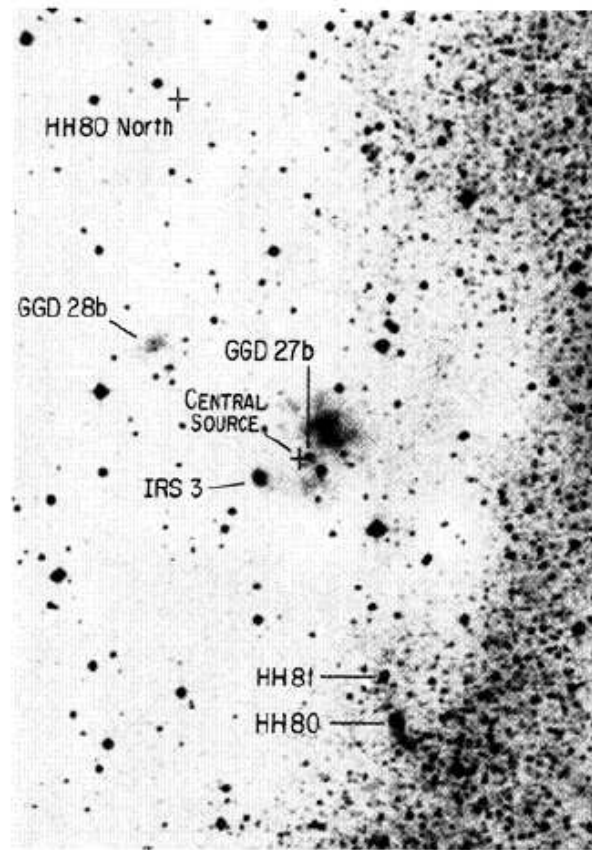


FIG. 1a

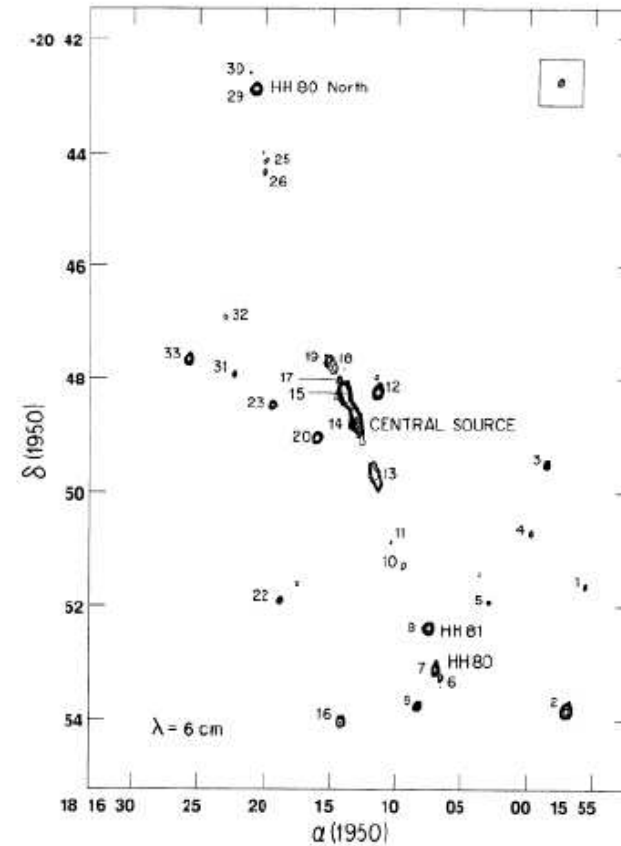
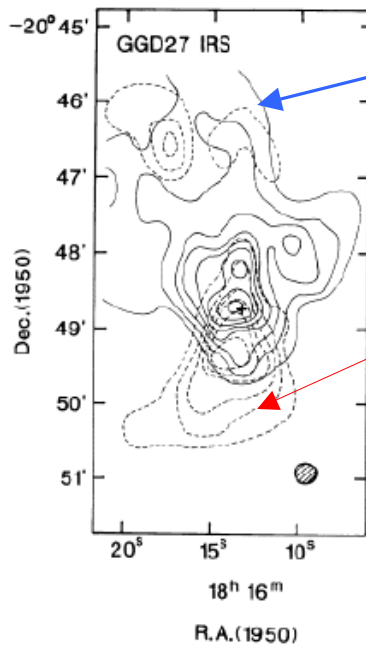


FIG. 1b

FIG. 1.—(a) The region of HH 80–81 and GGD 27–28 is seen in this figure from a deep red ESO Schmidt plate. The various objects in the region are identified. GGD 27b is a reflection nebula a few arcseconds from the central source. IRS 3 coincides with radio object 20. The crosses mark the positions of HH 80 North and the central exciting source, objects with no optical counterpart. North is up, and east is left. (b) Composite VLA 6 cm map of the HH 80–81 system made with natural weighting, showing the same region as (a). The two fields combined are not primary beam response-corrected. The northern counterpart of HH 80–81 is clearly visible at the top of the map. Note also the presence of small condensations between the central source and the HH objects following a slightly sinusoidal path. This can be interpreted as evidence of jet precession. Contours are $-3, 3, 4, 5, 7, 10, 20, 50,$ and 100 times $20 \mu\text{Jy}$ per beam, the rms noise of the individual maps. The beam size is 7.0×4.9 with position angle of -18° .

Highly collimated jet with extension of 5.3 pc ($11'$)
 (Martí, Rodríguez & Reipurth 1993)



CO (blue)

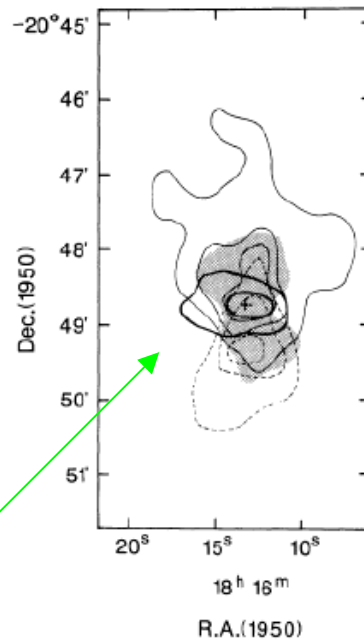
CO (red)

FIG. 2.—An angular distribution of the blueshifted ($V_{LSR} = 6-10.5 \text{ km s}^{-1}$) and the redshifted ($V_{LSR} = 14.5-19 \text{ km s}^{-1}$) wing components of the CO emission. The beam size is displayed in the right-hand lower corner. The contour interval is 2 K km s^{-1} .

(Yamashita et al. 1989)

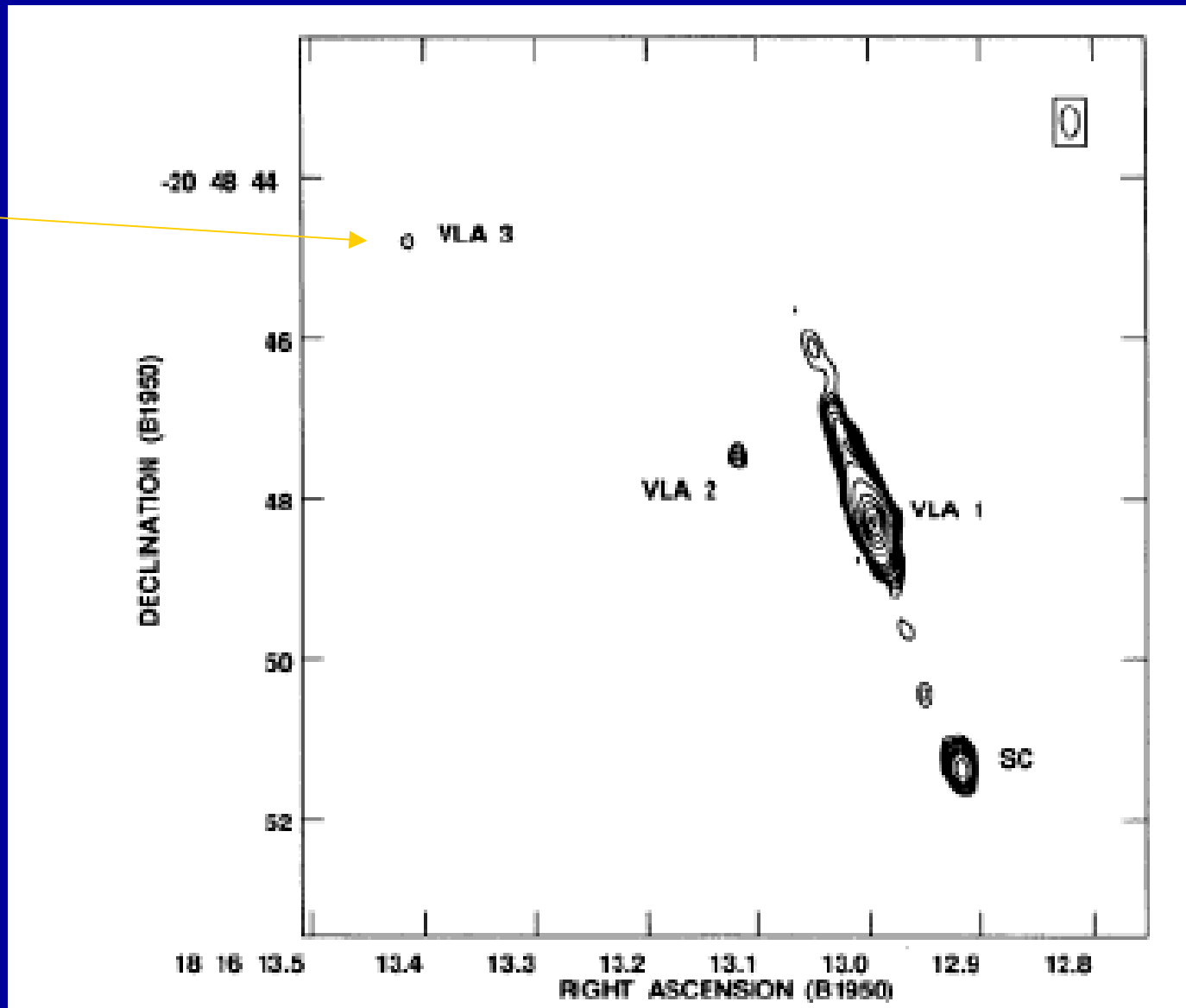
CS (2-1) torus

(Nobeyama 45m, $36''$ resolution)



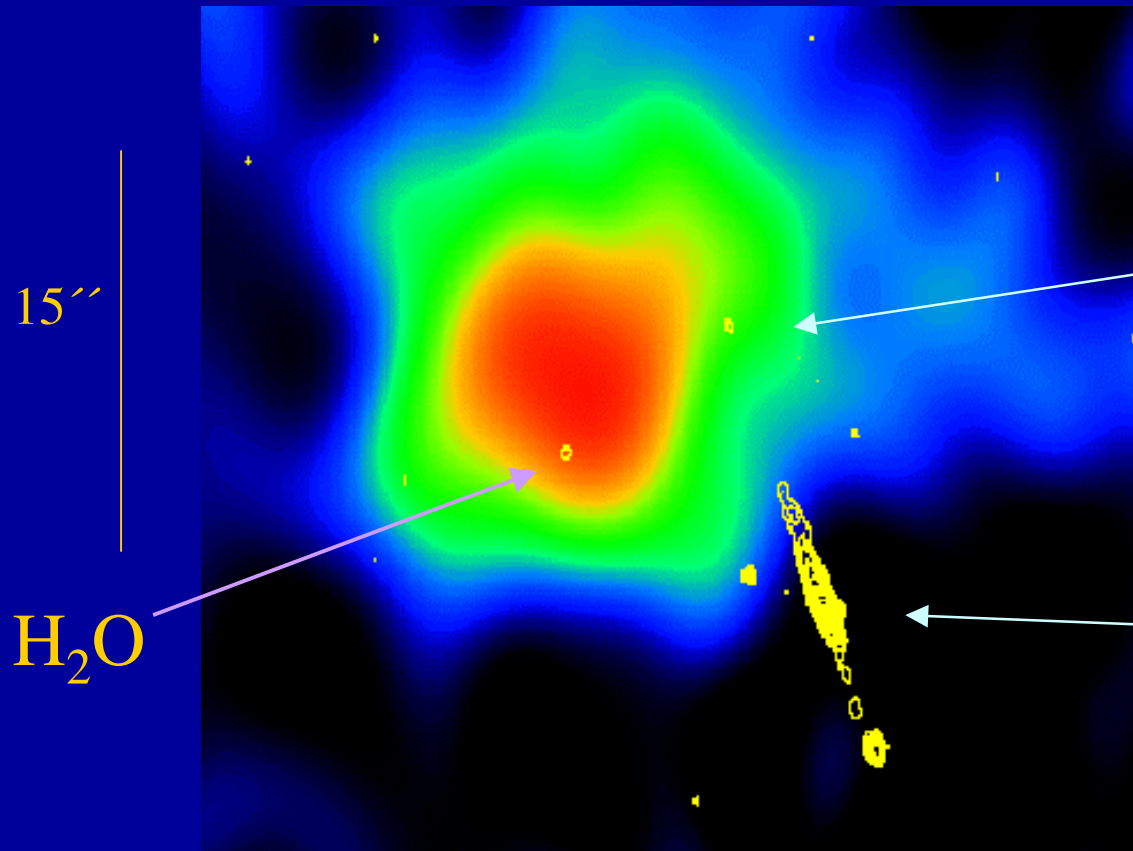
NO clear evidence of a disk in HH 80-81

H₂O
maser



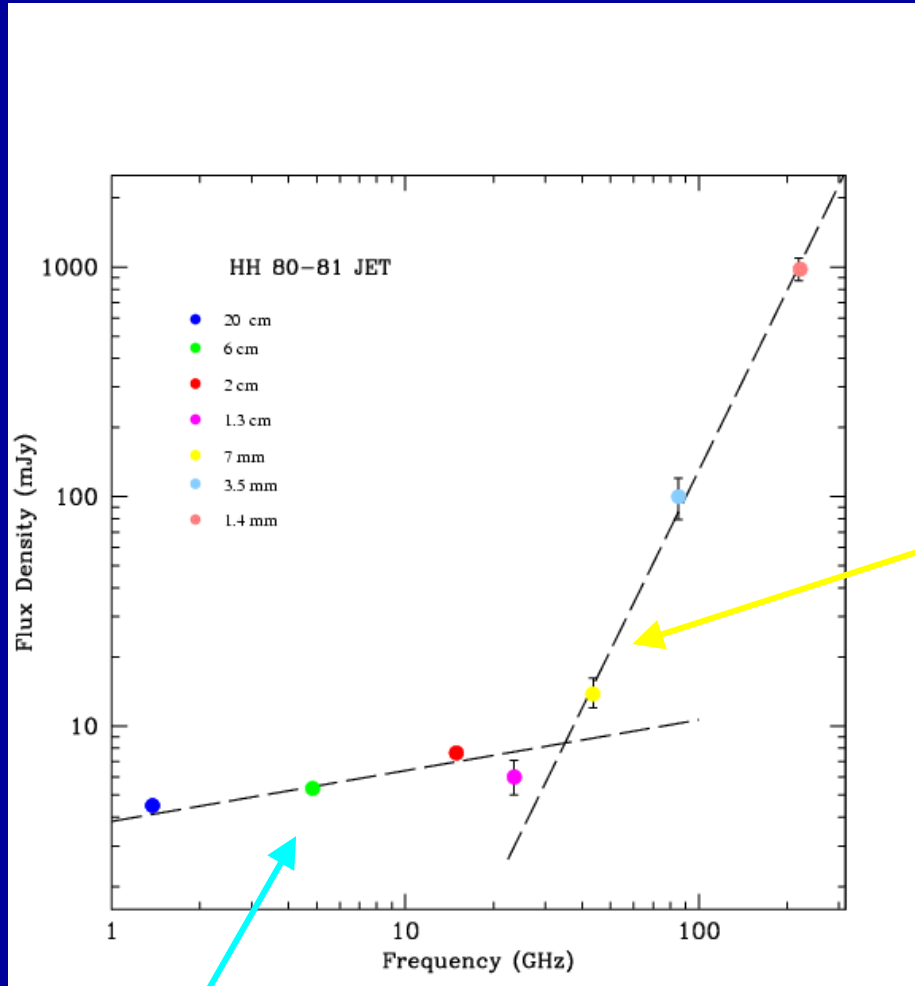
Gómez et al. 1995

Observations (1999):
VLA NH_3 (1,1) y (2,2)
Resolution $\sim 4''$ at 1.3 cm



NH_3 (1,1)

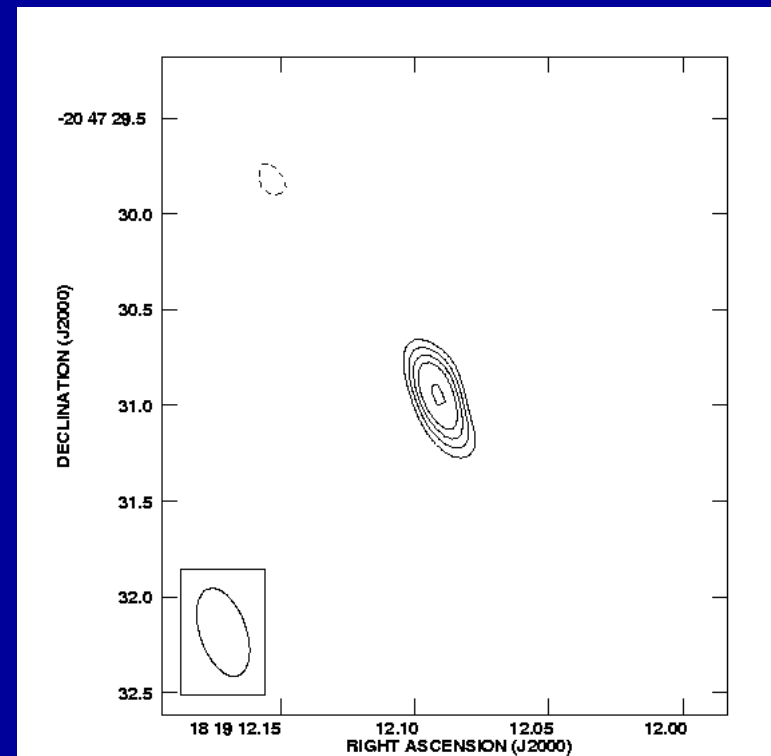
Continuum jet
at 3.6 cm

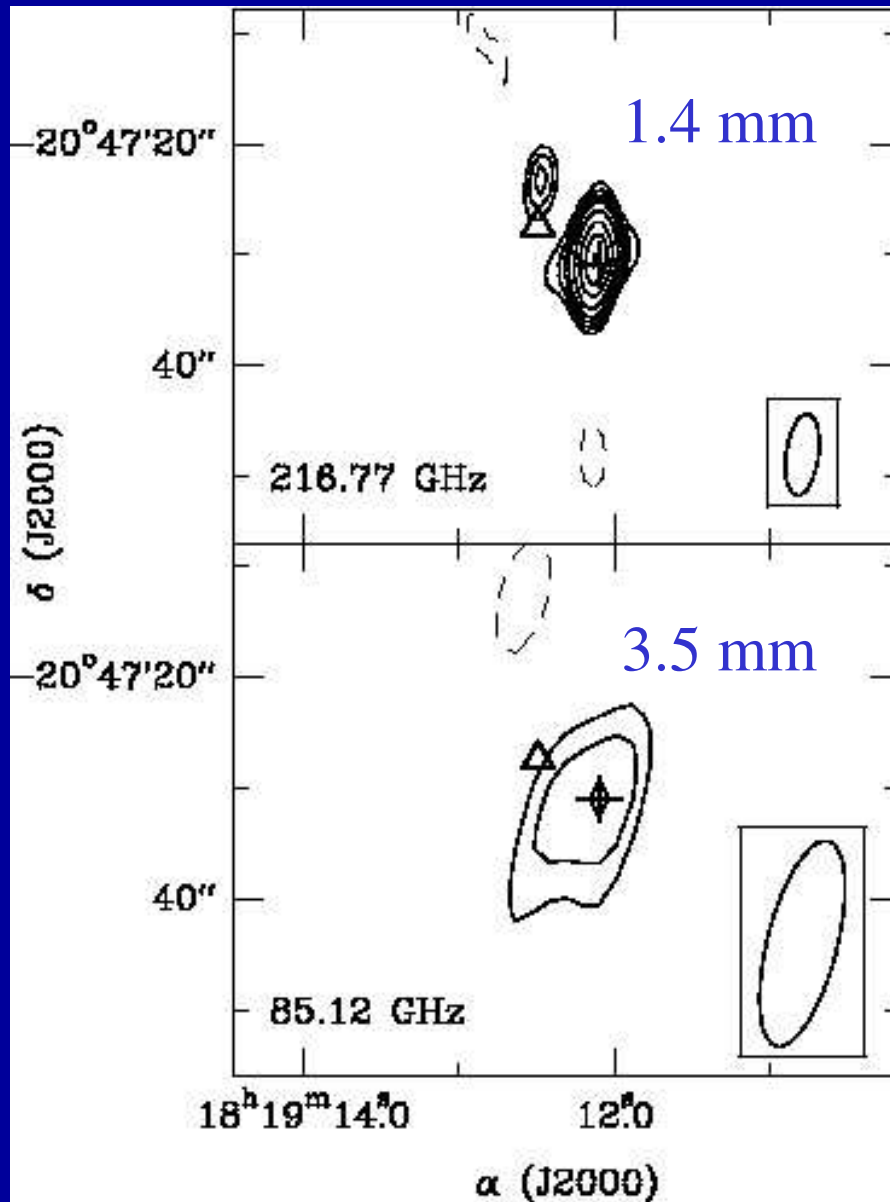


7 mm emission
observed with the
VLA at a
resolution of $0.4''$

Free-free $S_\nu \sim \nu^{+0.2}$

Gómez et al. 2003



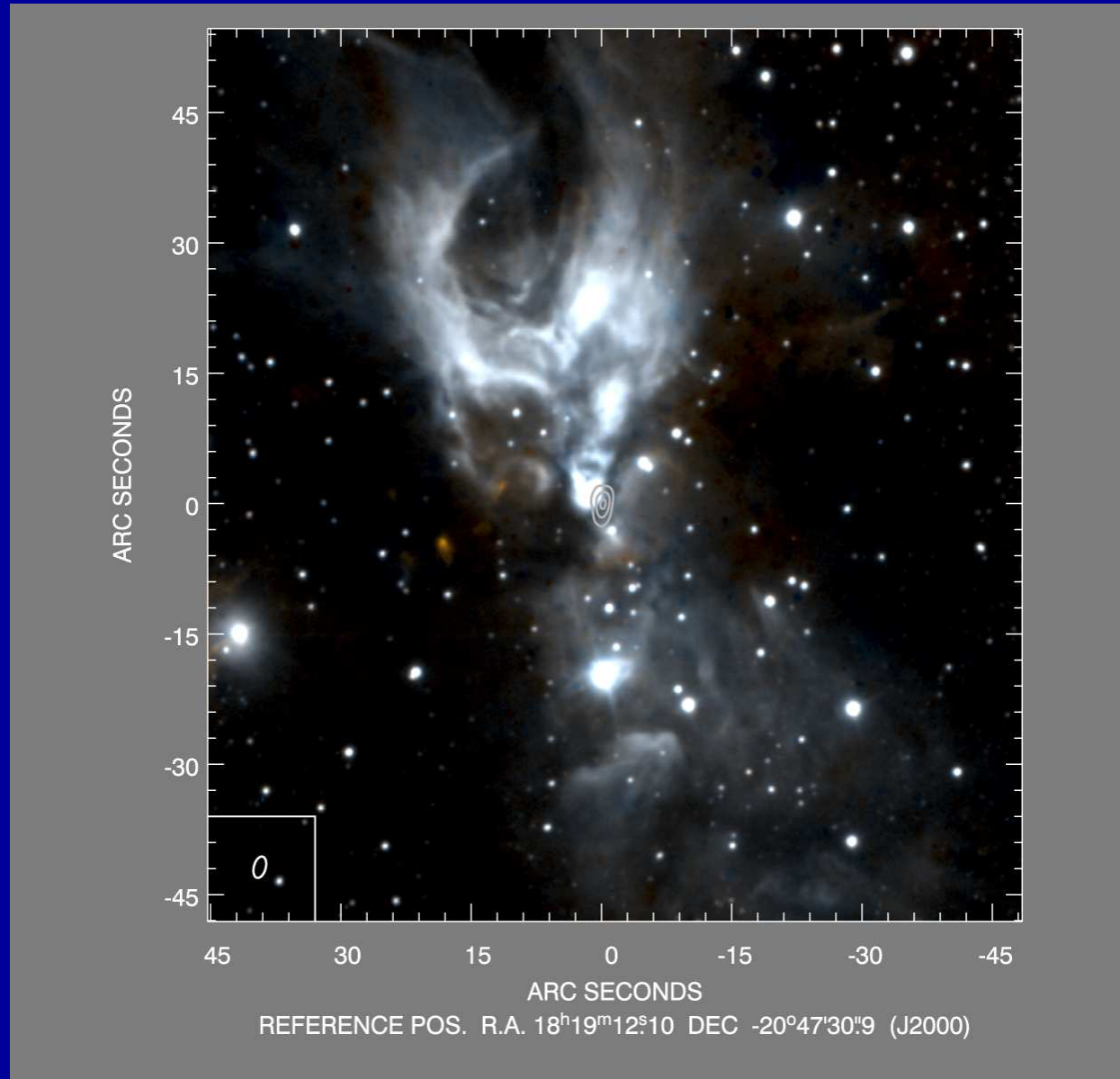


Continuum flux grows rapidly as $S_{\nu} \sim \nu^{2.6}$ suggesting dust emission.

Assuming dust emission is optically thin and temperature between 50-100 K, < total mass of $3.7 - 1.8 M_{\text{sol}}$ is derived following Beckwith & Sargent (1991).

BIMA

(resolutions of 7.4 y $19''$, respectively)



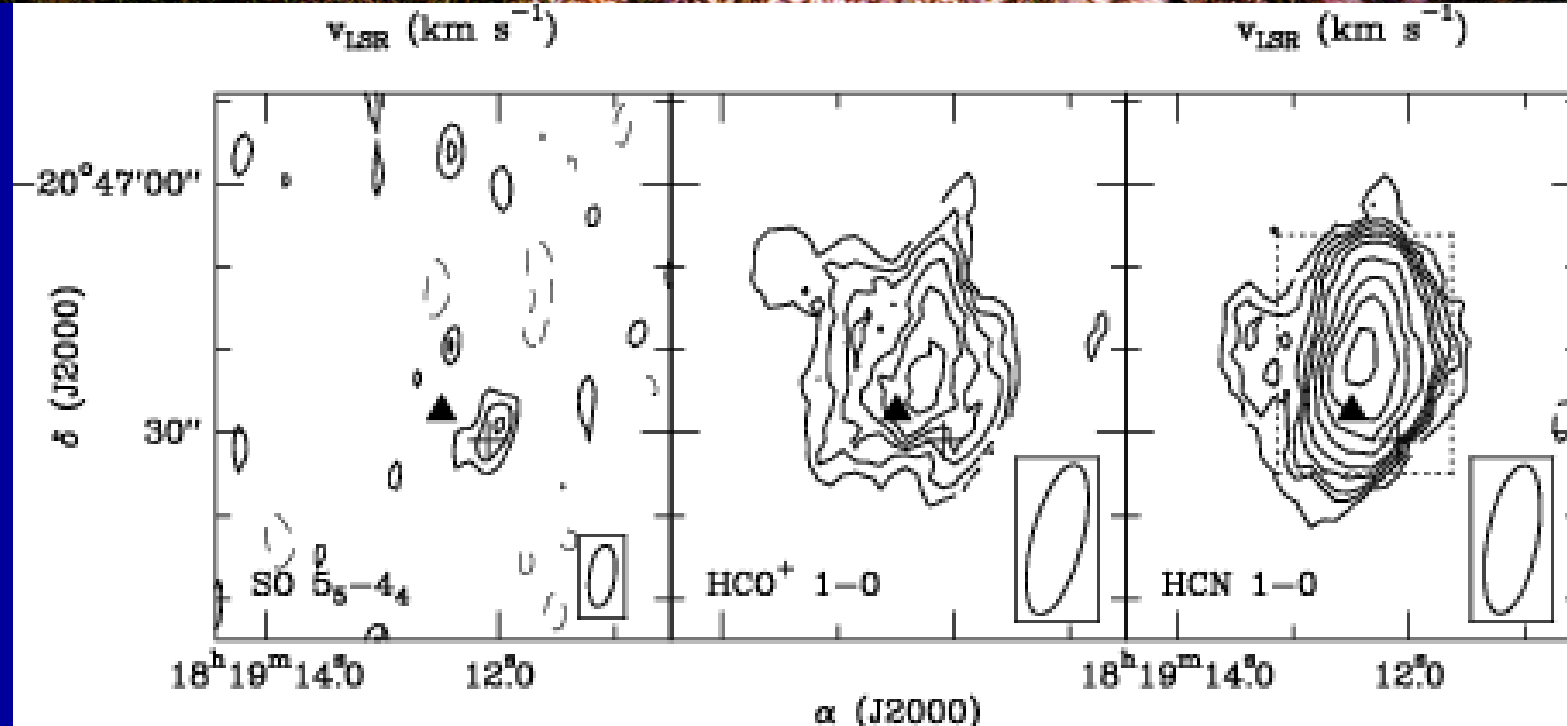
Blue=Br γ

Red= H₂

Contours:7mm
2.5''x1.5''

Linz, H., Hofner, P. & Stecklum 2003, in preparation

BIMA (1999 y 2001)



SO (5_5-4_4)

1.4 mm

HCO⁺ (1-0)

3.5 mm

HCN (1-0)

3.5 mm

SO emission coincides with exciting source of thermal jet, with angular size smaller than $5''$ or ~ 0.04 pc.

SO ($5_5 - 4_4$) traces hot (> 40 K) and dense ($\sim 10^6$ cm^{-3}) gas (Chernin et al. 1994).

From SO spectrum a column density of $N(\text{SO}) = 2.5 - 3.4 \times 10^{14} \text{ cm}^{-2}$ is derived for temperatures of $50 - 100$ K.

Assuming $[\text{SO}/\text{H}_2]$ of $0.5 - 2.0 \times 10^{-8}$ (Helmich & Dishoeck 1997) a mass of $0.7 - 3.5 M_{\text{sol}}$ is derived.

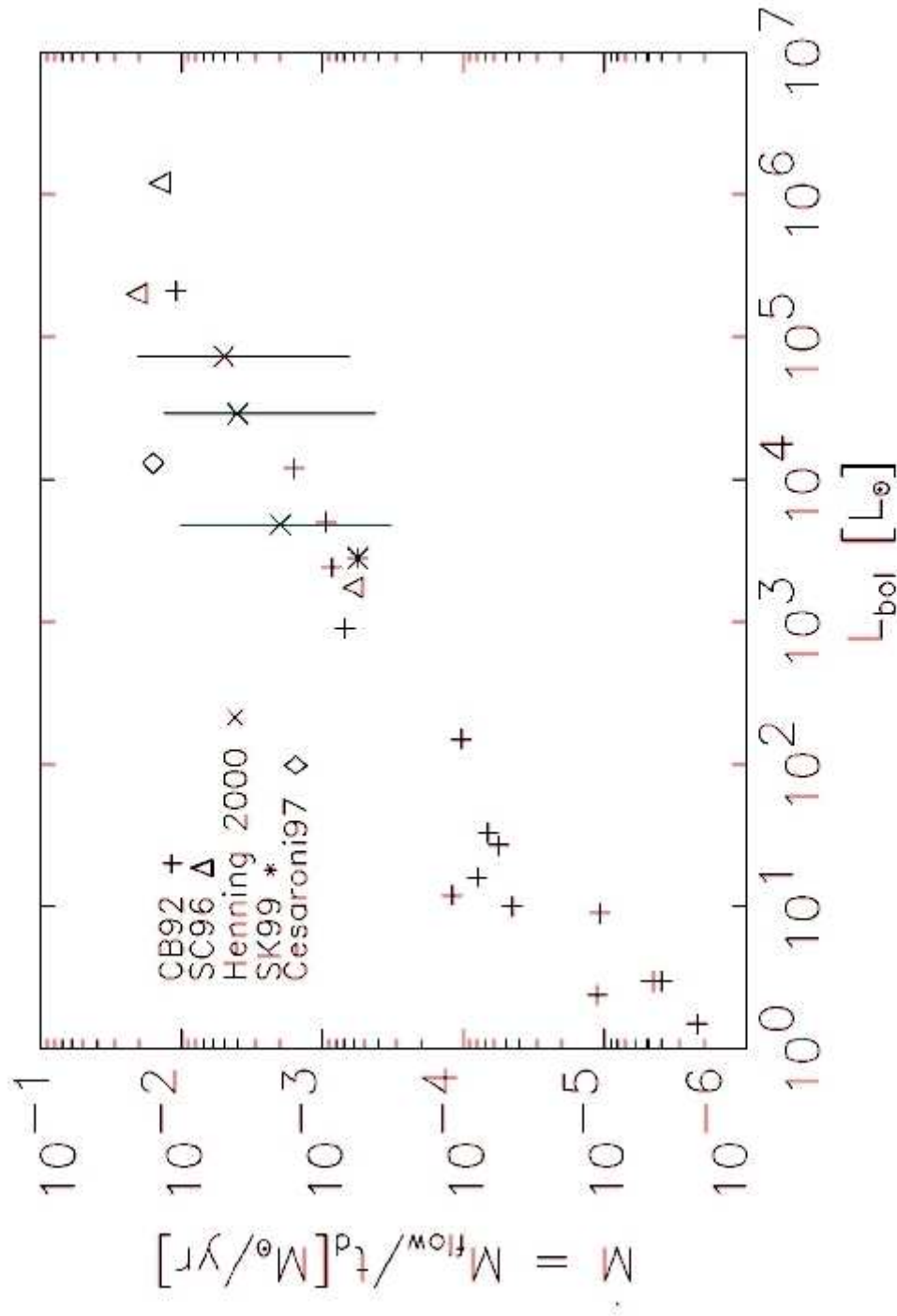
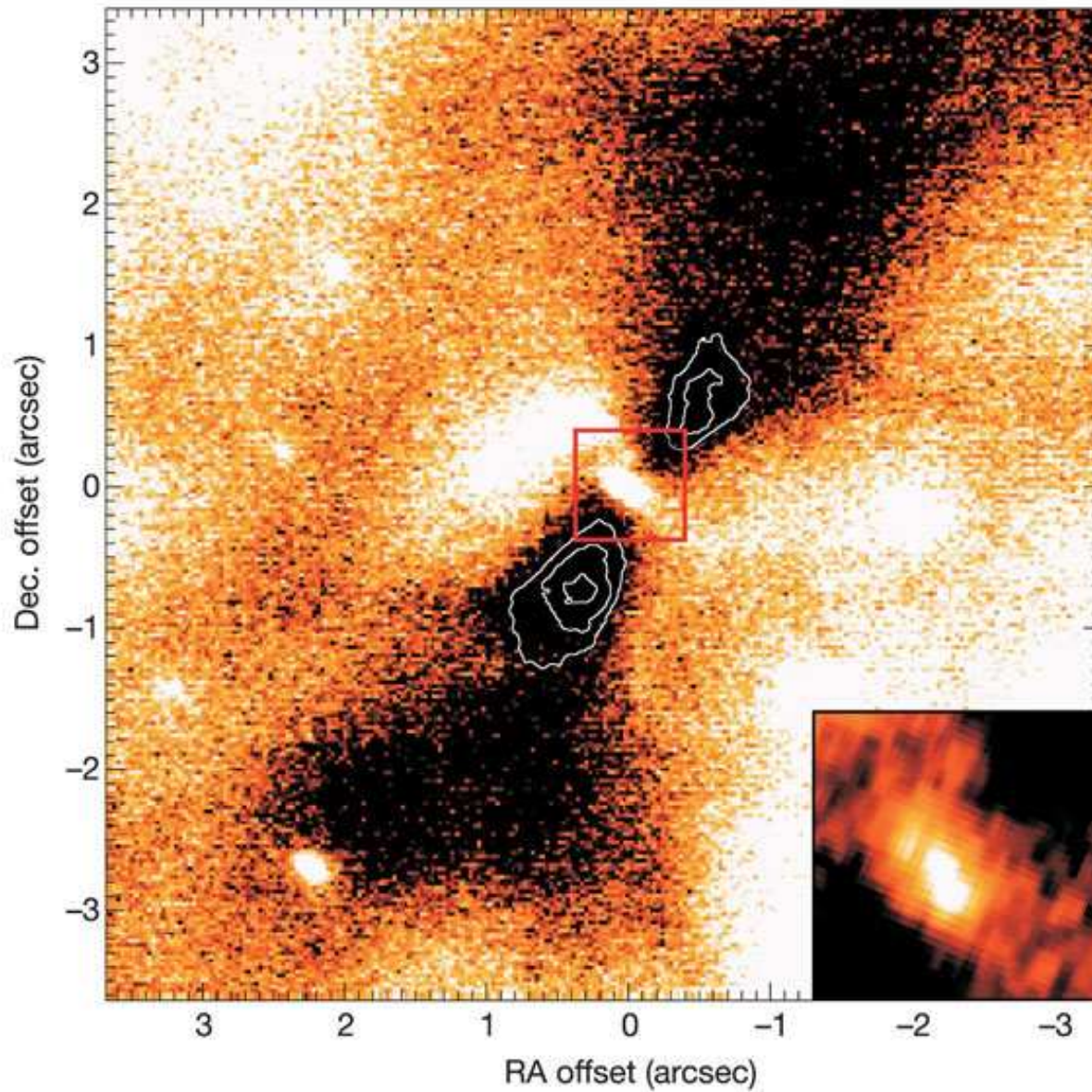


Figure 5 The mass outflow rate of bipolar molecular outflows driven by protostars of bolometric luminosity ranging from 1 to $10^6 M_{\odot} \text{yr}^{-1}$. Data for this plot were assembled from Cabrit & Bertout (1992), Shepherd & Churchwell (1996), Henning et al. (2000), Cesaroni et al. (1997), and Shepherd & Kurtz (1999).

Evidence for disks in massive stars very limited...

- NGC 7538 IRS1, HH 80-81, a few more sources...
- Let's look at case of a new source in M17 (Chini et al. 2004), at a distance of 2.2 kpc

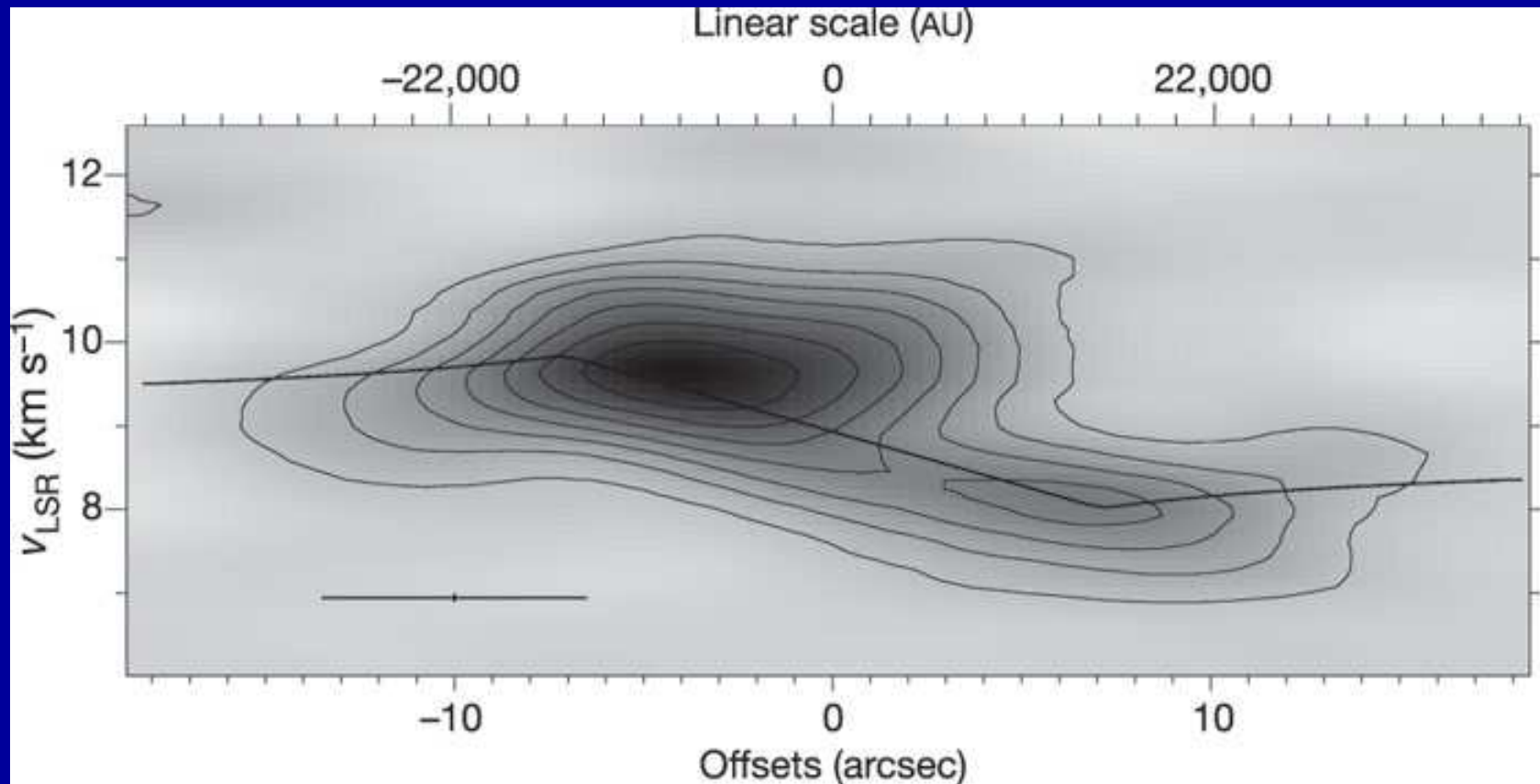


2.2 μm ESO's VLT

Seen in silhouette:

Dense inner torus
(2,000 AU in diameter)

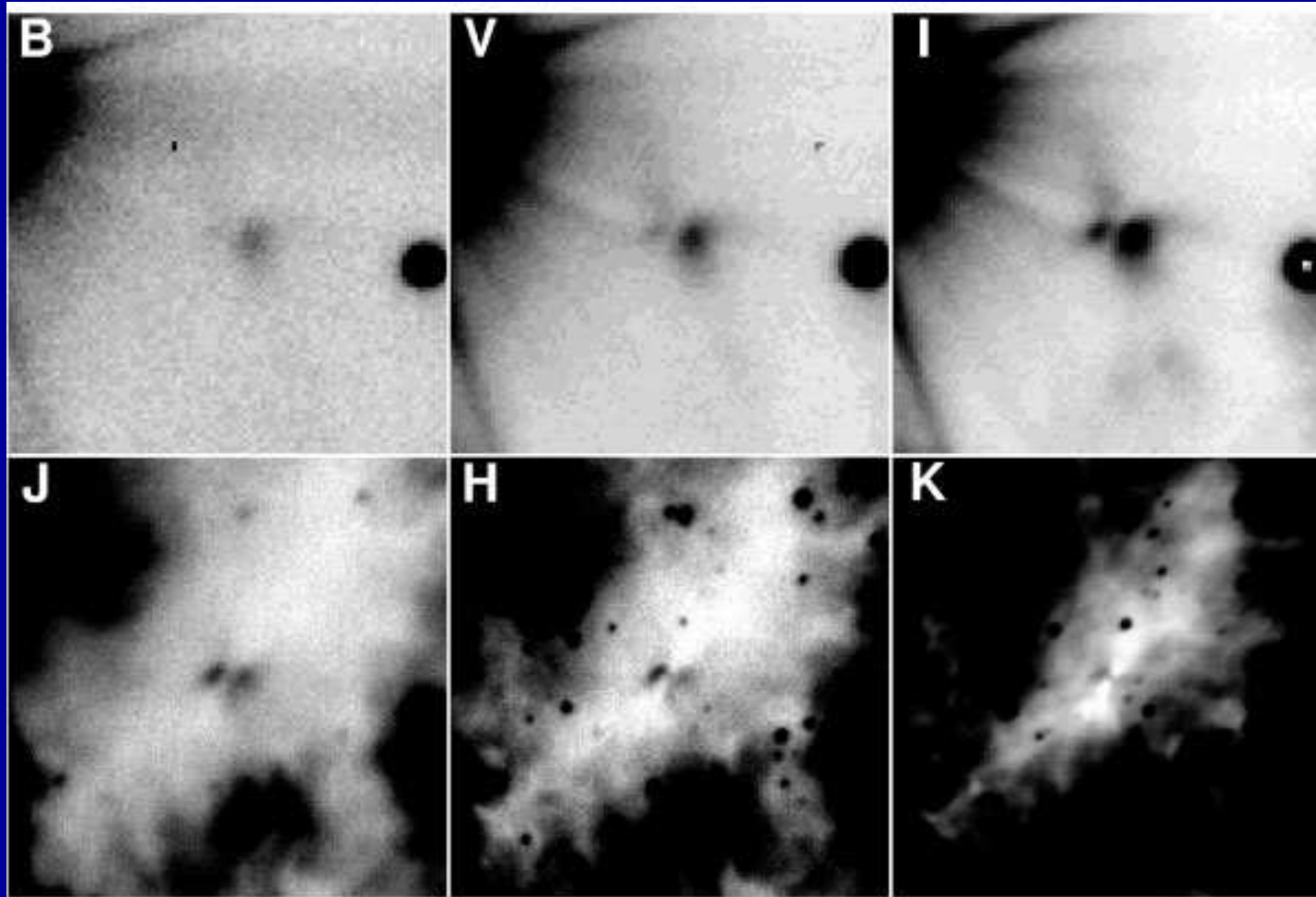
Flared disk about 10
times bigger



^{13}CO PdBI data

Velocity gradient across disk suggests central mass of $15 M_{\text{sun}}$

Mass in disk estimated to be $100 M_{\text{sun}}$



Central hourglass nebula marks the position of stars

Optical spectrum of hourglass nebula shows lines that in low mass stars are indicators of accretion, while shape suggestive of outflow

Finally, let's consider massive, prestellar molecular cores

- Only a handful know...
- Are low mass stars already formed in them (before high mass stars do)?
- Should look like HMCs, only that cold.

TABLE 2
DERIVED PARAMETERS

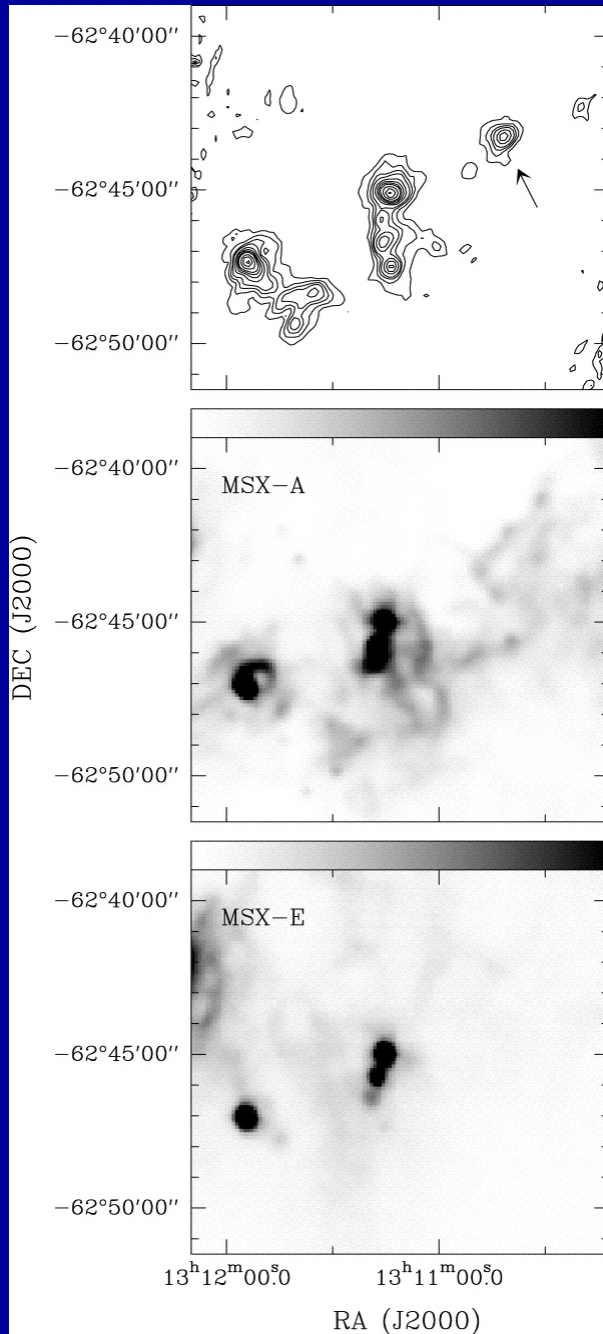
| SIMBA SOURCE (1) | D (kpc) (2) | 1.2 mm | | | | CS (2 → 1) | | |
|----------------------|---------------------|--------------------|---------------------|-------------------------------|--------------------------------------|--------------------|--|------------------------------------|
| | | R (pc) (3) | T_d (K) (4) | M^a (M_\odot) (5) | n^a (cm^{-3}) (6) | R (pc) (7) | M_{vir} (M_\odot) (8) | n (cm^{-3}) (9) |
| G305.136+0.068 | 3.4 | 0.27 | <16 | 1.1×10^3 | 2×10^5 | 0.30 | 1.1×10^3 | 2×10^5 |
| G333.125−0.562..... | 3.5 | 0.34 | <17 | 2.3×10^3 | 2×10^5 | 0.68 | 2.2×10^3 | 3×10^4 |
| G18.606−0.076..... | 3.7 | 0.20 | <15 | 4.0×10^2 | 2×10^5 | ... | ... | ... |
| G34.458+0.121 | 3.8 | 0.24 | <17 | 7.8×10^2 | 2×10^5 | 0.64 | 1.5×10^3 | 2×10^4 |

^a Lower limit.

Garay et al. (2004)

Massive but cold (and thus with low luminosity)

How are they found?



Garay et al (2004)

IRAS 13080-6229

1.2 mm, 8.8-10.8 μm , and 18.2-25.1 μm observations

Non detection at 8.8-10.8 μm and 18.2-25.1 μm implies low temperature

Many open questions in massive star formation...

- Accretion or mergers?
- Disks and jets?
- Do massive stars form always in the clustered mode or can they form alone?